ERROR ESTIMATES OF FINITE ELEMENT METHODS FOR NONLOCAL PROBLEMS USING EXACT OR APPROXIMATED INTERACTION NEIGHBORHOODS

QIANG DU, HEHU XIE, XIAOBO YIN, AND JIWEI ZHANG

ABSTRACT. We study the asymptotic error between the finite element solutions of nonlocal models with a bounded interaction neighborhood and the exact solution of the limiting local model. The limit corresponds to the case when the horizon parameter, the radius of the spherical nonlocal interaction neighborhood of the nonlocal model, and the mesh size simultaneously approach zero. Two important cases are discussed: one involving the original nonlocal models and the other for nonlocal models with polygonal approximations of the nonlocal interaction neighborhood. Results of numerical experiments are also reported to substantiate the theoretical studies.

1. INTRODUCTION

Nonlocal modeling has become popular in recent years among many applications [3, 9, 12, 30, 32]. As nonlocal integral operators are the key components of nonlocal modeling, their effective numerical integrations play important roles in both practice applications and numerical analysis. Our study here is devoted to this topic of wide interest. We focus on a model problem described below.

Let $\Omega \subset \mathbb{R}^d$ denote a bounded and open polyhedron. For $u_\delta(\mathbf{x}) : \Omega \to \mathbb{R}$, the nonlocal operator $\mathcal{L}_\delta$ on $u_\delta(\mathbf{x})$ is defined as

$$(1.1) \qquad \mathcal{L}_\delta u_\delta(\mathbf{x}) = 2 \int_{\mathbb{R}^d} \left(u_\delta(\mathbf{y}) - u_\delta(\mathbf{x}) \right) \gamma_\delta(\mathbf{x}, \mathbf{y}) d\mathbf{y} \quad \forall \mathbf{x} \in \Omega,$$

where the nonnegative symmetric mapping $\gamma_\delta(\mathbf{x}, \mathbf{y}) : \mathbb{R}^d \times \mathbb{R}^d \to \mathbb{R}$ is called a kernel. The operator $\mathcal{L}_\delta$ is regarded nonlocal since the value of $\mathcal{L}_\delta u_\delta$ at a point $\mathbf{x}$ involves information about u_δ at points $\mathbf{y} \neq \mathbf{x}$. In this paper, we consider the

Department of Applied Physics and Applied Mathematics, and Data Science Institute, Columbia University, NY 10027, USA (qd2125@columbia.edu).

LSEC, NCMIS, Academy of Mathematics and Systems Science, Chinese Academy of Sciences, Beijing 100190, & School of Mathematical Sciences, University of Chinese Academy of Sciences, Beijing, 100049, China (hhxie@lsec.cc.ac.cn).

School of Mathematics and Statistics, and Key Laboratory of Nonlinear Analysis & Applications (Ministry of Education), Central China Normal University, Wuhan 430079, China (yinxb@ccnu.edu.cn).

School of Mathematics and Statistics, and Hubei Key Laboratory of Computational Science, Wuhan University, Wuhan 430072, China (jiweizhang@whu.edu.cn).

following nonlocal Dirichlet volume-constrained diffusion problem

$$(1.2) \qquad \begin{cases} -\mathcal{L}_\delta u_\delta(\mathbf{x}) & = f_\delta(\mathbf{x}) \quad \text{on } \Omega, \\ \quad u_\delta(\mathbf{x}) & = g_\delta(\mathbf{x}) \quad \text{on } \Omega_\delta^c, \end{cases}$$

where $\Omega_\delta^c = \{ \mathbf{y} \in \mathbb{R}^d \setminus \Omega : \text{dist}(\mathbf{y}, \partial\Omega) < \delta \}$ denotes the interaction domain, f_δ and g_δ are given functions. For convenience, we denote by $\widehat{\Omega}_\delta = \Omega \cup \Omega_\delta^c$. Since interactions often occur over finite distances in real-world applications, we only consider kernels having bounded support, i.e., $\gamma_\delta(\mathbf{x}, \mathbf{y}) \neq 0$ only if $\mathbf{y}$ is within a neighborhood of $\mathbf{x}$. For this neighborhood, a popular practice is to choose a spherical domain, that is, a Euclidean ball $B_\delta(\mathbf{x})$ centered at $\mathbf{x}$ with a radius δ, i.e.,

$$(1.3) \qquad \text{for } \mathbf{x} \in \Omega : \ \gamma_\delta(\mathbf{x}, \mathbf{y}) = 0, \ \forall \mathbf{y} \in \mathbb{R}^d \setminus B_\delta(\mathbf{x}).$$

Here δ is known as the horizon parameter or the interaction radius. Volume constraints (VCs) imposed on Ω_δ^c are natural extensions to the nonlocal case of boundary conditions (BCs) for differential equation problems. While the Dirichlet case is given in (1.2) as an illustration, one can find discussions on other BCs, for example, nonlocal versions of Neumann and Robin BCs in [13, 16]. Along with (1.3), the kernel is further assumed to be radial, i.e. $\gamma_\delta(\mathbf{x}, \mathbf{y}) = \widetilde{\gamma}_\delta(|\mathbf{y} - \mathbf{x}|)$, with the following conditions being satisfied:

$$(1.4) \qquad \begin{cases} \widetilde{\gamma}_\delta(s) > 0 \ \text{for} \ 0 < s < \delta, \\ \widetilde{\gamma}_\delta(s) \in L^1(0, \delta), \\ w_d \int_0^\delta s^{d+1} \widetilde{\gamma}_\delta(s) ds = d, \end{cases}$$

where w_d is the surface area of the unit sphere in $\mathbb{R}^d$. The radial symmetry of $\gamma_\delta(\mathbf{x}, \mathbf{y})$ matches with the choice of the spherical interaction neighborhood. Note that the first condition of (1.4) means that the kernel is strictly positive for $\mathbf{y}$ inside $B_\delta(\mathbf{x})$. The second condition is a simplifying assumption, which implies that $\mathcal{L}_\delta$ is a bounded operator in L^2. The third condition of (1.4) is set to ensure that if the operator $\mathcal{L}_\delta$ converges to a limit as $\delta \to 0$, then the limit is given by $\mathcal{L}_0 = \Delta$, the classical diffusion operator, see related discussions in [35, 36]. To be specific, if the corresponding local problem is defined as follows:

$$(1.5) \qquad \begin{cases} -\mathcal{L}_0 u_0(\mathbf{x}) & = f_0(\mathbf{x}) \quad \text{on } \Omega, \\ \quad u_0(\mathbf{x}) & = g_0(\mathbf{x}) \quad \text{on } \partial\Omega. \end{cases}$$

Then the third condition of (1.4) implies that as $\delta \to 0$, the nonlocal effect dimin-

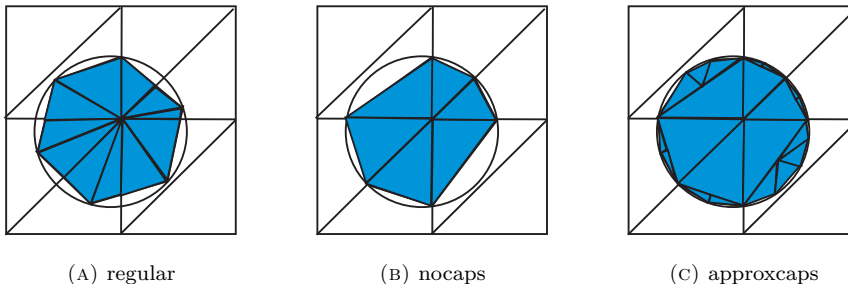(A) regular   (B) nocaps   (C) approxcaps

FIGURE 1. Polygonally approximated balls, taken from [17]

ishes and if the solutions of nonlocal equations converge, the limit is given by the solution of a classical local differential equation. Such a limiting property can serve to connect nonlocal and local models and is of great significance for practical application, e.g., multiscale modeling and benchmark testing. It is an important issue of numerical analysis to investigate the extent of preserving this limiting property on the discrete level for various discrete approximations. Motivated by the findings in [6, 7, 10, 34] that the numerical solutions based on the piecewise constant finite element methods (FEMs) fail to converge to a physically consistent local limit if the ratio of δ and h (mesh size) is fixed, Tian and Du [35] proposed the concept of asymptotically compatible (AC) schemes for the numerical approximations of a broad class of parametrized problems which, for nonlocal problems under consideration, are convergent discrete approximation schemes of the nonlocal models that preserve the correct local limiting behavior. In other words, the numerical approximation given by an AC scheme can also reproduce the correct local limiting solution as the horizon parameter and the mesh size approach zero free of the relationship between them. They lead to consistent numerical results for benchmark problems without the need for a fine-tuning of model and discretization parameters, δ and h, and thus are regarded as more robust and more suitable for simulating problems involving nonlocal interactions on multiple scales such as in peridynamics [4]. In [35], it was revealed that under very general assumptions on the problems, as long as the finite element space contains continuous piecewise linear functions, the Galerkin finite element approximation is always AC. However, the method using piecewise constant finite element is only a conditionally AC scheme under the condition that $\delta = o(h)$ [7, 10, 35]. In [7], one can find similar discussions, using numerical experiments, on the convergence in different regimes of the parameters δ and h.

It is worth noting that most of the existing studies were carried out under the assumption that all the integrals involved are computed exactly. The latter could be demanding, thus requiring careful consideration in practice [41, 27]. One important cause is due to the choice of the nonlocal interaction neighborhood of the operator $\mathcal{L}_\delta$ defined in (1.1) being confined to Euclidean balls. For finite element methods based on polyhedral meshes, dealing with intersections of such balls and mesh elements leads to considerable challenges in numerical implementation. As possible alternatives, the integrals may be approximated by truncation of the interaction neighborhoods, or by numerical integration, or a combination of both. For example, D'Elia et. al. [11] discussed several geometric approximations of the Euclidean balls in 2D (like *regular*, *nocaps* and *approxcaps* approximations, see Figure 1). They showed how such approximations, in combination with quadrature rules, affect the discretization error. They also provided numerical realization which shows that some geometric approximations preserve optimal accuracy in approximating the nonlocal solution under the assumption that the horizon parameter is fixed. However, when the AC property is concerned, the conclusion is different. It is revealed in [17] that all types of polygonal approximations considered in [11] lose the desirable AC property even when they are used in the context of an AC scheme with exact integration. In other words, the numerical solutions of nonlocal problems with polygonal approximations may fail to converge to the right local limit. On the other hand, the AC property can hold conditionally which means they could be used with certain restrictions.

The discussion in [17] was carried out on the continuum level, focused only on the approximations of the interaction neighborhoods. The conclusions are mostly qualitative. Thus, quantitative analysis on both continuum and discrete levels remains an interesting issue, which provides the key motivation and the first objective of this study. In fact, even for the FEM taking Euclidean balls as supports of nonlocal interaction kernels, there have been limited derivations of rigorous error estimates with respect to the horizon parameter and mesh size. Moreover, there has been no theoretical attempt to analyze the convergence of numerical approximations of peridynamic models where the spherical support of the kernel is polygonally approximated. The same observation can also be made in the case of meshfree methods when partial interaction volumes and geometric centers of intersecting regions are not precisely calculated. In contrast, it is worth mentioning that in [18] for Fourier spectral methods of nonlocal Allen-Cahn equation for 1D in space with periodic BCs, error estimates with respect to horizon parameter and Fourier parameter have been rigorously derived for smooth local solutions.

As the second objective of this work, we study the convergence property of nonlocal solutions and their finite element approximations in both energy and L^2 norms. Recall the analog for the local PDE setting: the error in the energy norm is first derived, followed by the Aubin-Nitsche technique, which leads to the error estimate in the L^2 norm. Unfortunately, due to the possible lack of elliptic smoothing property, the L^2 error estimate remained in the same order as the estimate in the nonlocal energy norm if the horizon parameter is fixed. A natural question is how the Aubin-Nitsche theory behaves if the dependence of the horizon parameter is considered.

In this work, the error estimates are derived using the following triangle inequality:

$$(1.6) \qquad \left\| u_\sharp^h - \widetilde{u}_0 \right\|_\sharp \le \left\| u_\sharp - \widetilde{u}_0 \right\|_\sharp + \left\| u_\sharp - u_\sharp^h \right\|_\sharp := E_1 + E_2,$$

$$(1.7) \qquad \left\| u_\sharp^h - u_0 \right\|_{L^2(\Omega)} \le \left\| u_\sharp - u_0 \right\|_{L^2(\Omega)} + \left\| u_\sharp - u_\sharp^h \right\|_{L^2(\Omega)}.$$

Here, $\widetilde{u}_0$ is the C^4 extension of u_0 as defined in definition 2.1, see also [20, 38]. Here the symbol $\sharp$ is used to identify the solution or the energy norm associated with one of the following two cases

$$(1.8) \qquad \qquad \{\sharp = \delta; \ \sharp = (\delta, n_\delta)\}.$$

The two cases identified by $\sharp$ correspond respectively to nonlocal solutions and the energy norms associated with interaction neighborhoods given by Euclidean balls and non-symmetric polygons with n_δ being the maximum number of polygons' sides.

Concerning the energy norm $\|\cdot\|_\sharp$, the first part E_1 has the estimate

$$E_1 = \begin{cases} \|u_\delta - \widetilde{u}_0\|_\delta & \lesssim \delta^{(3+\mu)/2}, \\ \|u_{\delta,n_\delta} - \widetilde{u}_0\|_{\delta,n_\delta} & \lesssim \delta^{(3+\mu)/2} + \delta^{-1} n_\delta^{-\lambda}, \end{cases}$$

for $\lambda = 2$ or 4 with the value depending on the kernel, see (2.15). In this part, we also derive the estimate for another interesting case, $\sharp = (\delta|n_\delta)$, with the interaction neighborhoods given by symmetric polygons and the estimate of the form

$$\|u_{\delta|n_\delta} - \widetilde{u}_0\|_\delta \lesssim \delta^{(3+\mu)/2} + n_\delta^{-\lambda}.$$

One may observe that the error of u_{δ,n_δ} against the local solution is one order lower than that of $u_{\delta|n_\delta}$ with respect to δ. To offer an explanation, we notice that for sufficiently smooth $\widetilde{u}_0$,

$$\mathcal{L}_{\delta,n_\delta}\widetilde{u}_0(\mathbf{x}) = F(\mathbf{x}) + \sum_{i=1}^{2} \sigma_{n_\delta}^{ii,2}(\mathbf{x})\partial_{ii}\widetilde{u}_0(\mathbf{x}) + O\left(\delta^2\right),$$

where, due to the non-symmetric nature of the effective interaction domain, $F(\mathbf{x})$ contains the odd moments up to the third-order and the second-order mixed moment of kernel γ_{δ,n_δ} while the dominant term is given by the first-order moment. In contrast, $\mathcal{L}_{\delta|n_\delta}\widetilde{u}_0(\mathbf{x})$ does not contain any term like $F(\mathbf{x})$, since the support of its kernel is symmetric with respect to $\mathbf{x}$. In fact, we have $|F(\mathbf{x})| \lesssim \delta^{-1} n_\delta^{-\lambda}$, which contributes to the extra error term of the error estimate in the non-symmetric case.

The second part E_2 is derived using the Cea's lemma in the nonlocal setting and the triangle inequality (see (3.13) for $\sharp = \delta$, and (3.21) for $\sharp = \delta, n_\delta$) as

$$E_2 = \left\| u_\sharp - u_\sharp^h \right\|_\sharp \leq \left\| u_\sharp - u_\sharp^* \right\|_\sharp + \left\| u_\sharp^* - u_\sharp^h \right\|_\sharp \leq \left\| u_\sharp - u_\sharp^* \right\|_\sharp + \left\| u_\sharp^* - I_h\widetilde{u}_0 \right\|_\sharp$$

$$\leq \left\| u_\sharp - u_\sharp^* \right\|_\sharp + \left\| u_\sharp^* - u_\sharp \right\|_\sharp + \left\| u_\sharp - \widetilde{u}_0 \right\|_\sharp + \left\| \widetilde{u}_0 - I_h\widetilde{u}_0 \right\|_\sharp$$

$$= 2 \left\| u_\sharp - u_\sharp^* \right\|_\sharp + \left\| \widetilde{u}_0 - I_h\widetilde{u}_0 \right\|_\sharp + \left\| u_\sharp - \widetilde{u}_0 \right\|_\sharp$$

$$\leq C\delta^{-1/2}h^2 + C\delta^{-1} \left\| \widetilde{u}_0 - I_h\widetilde{u}_0 \right\|_{C(\widehat{\Omega}_\delta)} + \left\| u_\sharp - \widetilde{u}_0 \right\|_\sharp$$

$$\leq C\delta^{-1/2}h^2 + C\delta^{-1}h^2 \left\| \widetilde{u}_0 \right\|_{C^2(\widehat{\Omega}_\delta)} + \left\| u_\sharp - \widetilde{u}_0 \right\|_\sharp$$

$$\lesssim \delta^{-1}h^2 + \left\| u_\sharp - \widetilde{u}_0 \right\|_\sharp.$$

Thus we obtain the total error estimate

$$\begin{cases} \|u_\delta^h - \widetilde{u}_0\|_\delta & \lesssim \delta^{(3+\mu)/2} + \delta^{-1}h^2, \\ \|u_{\delta,n_\delta}^h - \widetilde{u}_0\|_{\delta,n_\delta} & \lesssim \delta^{(3+\mu)/2} + \delta^{-1}h^2 + \delta^{-\lambda-1}h^\lambda, \end{cases}$$

under assumptions on the regularity of the local solution, but not on that of the nonlocal solution, see Theorems 4.1 and 4.2. A key contribution in this regard is the derivation of explicit error estimates with respect to the horizon parameter and the mesh size for finite element solutions of nonlocal problems under mild assumptions. The sharpness of the error estimate in the energy norm is verified in Section 5. This further offers confidence in using the estimates to guide numerical simulations of problems like the numerical simulations of peridynamics.

While the error estimate in the L^2 norm can be derived, via the Poincaré's inequality, from the error in the energy norm, such a result is generally not sharp as shown in Section 5. Naturally, if a nonlocal analog of Aubin-Nitsche theory for FEM of the local problem (Aubin [5] and Nitsche [26]) could be developed, then improved estimates of the error in the L^2 norm would be feasible, that is, an estimate of the form

$$\begin{cases} \|u_\delta^h - u_0\|_{L^2(\Omega)} & \lesssim \delta^2 + h^2, \\ \|u_{\delta,n_\delta}^h - u_0\|_{L^2(\Omega)} & \lesssim \delta^2 + h^2 + \delta^{-\lambda}h^\lambda, \end{cases}$$

might be expected. While the theoretical analysis is missing at the moment, it is verified numerically in Section 5. Based on the reported error estimates there, one can directly assess the convergence of the computed nonlocal solutions to the correct local limit for different choices of δ and h.

The rest of the paper is organized as follows. In Section 2, error estimates of the nonlocal solutions with different kernels against the local counterpart (E_1) are derived in terms of horizon parameter and, for the second case of (1.8), the maximum number of sides of polygons. Next, we study the error between the nonlocal solutions and their finite element approximations (E_2) in terms of horizon parameter and mesh size, and for the second case of (1.8), the maximum number of polygons's sides in Section 3. In Section 4, the error estimates in Section 2 are combined with that in Section 3 to obtain bounds of the error between the nonlocal discrete solutions and the local exact solution. Results of numerical experiments are reported in Section 5 to substantiate the theoretical studies. Finally, we give some concluding remarks in Section 6.

2. Convergence of the nonlocal solutions to the local limit

As in [13], the nonlocal energy inner product, nonlocal energy norm, nonlocal energy space, and nonlocal constrained energy subspaces are defined by

$$(u,v)_\delta := \int_{\widehat{\Omega}_\delta} \int_{\widehat{\Omega}_\delta} (u(\mathbf{y}) - u(\mathbf{x}))(v(\mathbf{y}) - v(\mathbf{x})) \gamma_\delta(\mathbf{x},\mathbf{y}) d\mathbf{y}d\mathbf{x}, \quad \|u\|_\delta := (u,u)_\delta^{1/2},$$

$$V(\widehat{\Omega}_\delta) := \left\{ u \in L^2(\widehat{\Omega}_\delta) : u(\mathbf{x}) = g_\delta(\mathbf{x}) \text{ on } \Omega_\delta^c, \|u\|_\delta < \infty \right\},$$

$$V^0(\widehat{\Omega}_\delta) := \left\{ u \in V(\widehat{\Omega}_\delta) : u(\mathbf{x}) = 0 \text{ on } \Omega_\delta^c \right\},$$

$$V^c(\widehat{\Omega}_\delta) := \left\{ u \in V(\widehat{\Omega}_\delta) : u(\mathbf{x}) = 0 \text{ on } \Omega \right\},$$

respectively. For a bounded domain $D \subset \mathbb{R}^d$, the space of bounded and continuous functions is denoted by $C_b(D) := \left\{ u \in C(D) : u \text{ is bounded on } \overline{D} \right\}$. For any non-negative integer n, we define

$$C_b^n(D) := \left\{ u \in C_b(D) : \forall \text{ non-negative integer } j \leq n, u^{(j)} \in C_b(D) \right\}.$$

Definition 2.1. For any function u defined on Ω, we let $\widetilde{u}$ be a C^n extension of u such that $\widetilde{u} \in C_b^n(\widehat{\Omega}_\delta)$ and $\widetilde{u}|_\Omega = u$, see also Definition 4.1 in [38].

2.1. **Convergence of the nonlocal solutions to the local limit.** In this subsection, we investigate for what kind of VCs, the nonlocal solutions of (1.2) converge to the local solution of (1.5), and with what asymptotic rate with respect to δ.

Theorem 2.2. *Suppose $u_0 \in C_b^4(\Omega)$ is the solution of the local problem (1.5), the family of kernels $\{\gamma_\delta\}$ satisfies (1.3), (1.4), and*

$$(2.1) \qquad\qquad G(\gamma_\delta) := \sup_{\mathbf{x} \in \widehat{\Omega}_\delta} \int_{B_\delta(\mathbf{x}) \cap \widehat{\Omega}_\delta} \gamma_\delta(\mathbf{x},\mathbf{y}) d\mathbf{y} \lesssim \delta^{-2}.$$

Let u_δ be the solution of the nonlocal problem (1.2). If $\widetilde{u}_0$ is a C^4 extension of u_0 and

$$(2.2) \qquad \|f_\delta - f_0\|_{C(\Omega)} = O\left(\delta^2\right), \quad \|g_\delta - \widetilde{u}_0\|_{C(\Omega_\delta^c)} = O\left(\delta^{2+\mu}\right), \ \mu = 0,1,$$

then it holds that

$$(2.3) \qquad \|u_\delta - u_0\|_{C(\Omega)} = O\left(\delta^2\right), \quad \|u_\delta - \widetilde{u}_0\|_\delta = O\left(\delta^{(3+\mu)/2}\right).$$

Proof. Since $\widetilde{u}_0 \in C_b^4(\widehat{\Omega}_\delta)$, a direct calculation leads to

$$-\mathcal{L}_\delta \widetilde{u}_0(\mathbf{x}) = -\mathcal{L}_0 u_0(\mathbf{x}) + O\left(\delta^2\right) |\widetilde{u}_0|_{4,\infty,\widehat{\Omega}_\delta} = f_0(\mathbf{x}) + O\left(\delta^2\right), \ \forall \mathbf{x} \in \Omega.$$

Thus, together with (2.2) it holds that

$$(2.4) \qquad \begin{cases} -\mathcal{L}_\delta\left(u_\delta - \widetilde{u}_0\right)(\mathbf{x}) = O\left(\delta^2\right), & \mathbf{x} \in \Omega, \\ u_\delta(\mathbf{x}) - \widetilde{u}_0(\mathbf{x}) = g_\delta(\mathbf{x}) - \widetilde{u}_0(\mathbf{x}) = O\left(\delta^{2+\mu}\right), & \mathbf{x} \in \Omega_\delta^c. \end{cases}$$

The application of nonlocal maximum principle [20, 33, 38, 39] to (2.4) produces

$$\|u_\delta - u_0\|_{C(\Omega)} = \|u_\delta - \widetilde{u}_0\|_{C(\Omega)} = O\left(\delta^2\right).$$

This, together with (2.1), (2.2), and (2.4), leads to

$$\|u_\delta - \widetilde{u}_0\|_\delta^2 = -\int_\Omega \left(u_\delta(\mathbf{x}) - u_0(\mathbf{x})\right) \mathcal{L}_\delta\left(u_\delta(\mathbf{x}) - \widetilde{u}_0(\mathbf{x})\right) d\mathbf{x}$$

$$- \int_{\Omega_\delta^c} \left(g_\delta(\mathbf{x}) - \widetilde{u}_0(\mathbf{x})\right) \int_{\widehat{\Omega}_\delta} \left(u_\delta(\mathbf{y}) - \widetilde{u}_0(\mathbf{y}) - g_\delta(\mathbf{x}) + \widetilde{u}_0(\mathbf{x})\right) \gamma_\delta(\mathbf{x},\mathbf{y}) d\mathbf{y} d\mathbf{x}$$

$$\lesssim \delta^4 + |\Omega_\delta^c| \cdot \|g_\delta - \widetilde{u}_0\|_{C(\Omega_\delta^c)} \cdot \left(\|u_\delta - u_0\|_{C(\Omega)} + \|g_\delta - \widetilde{u}_0\|_{C(\Omega_\delta^c)}\right) \cdot G(\gamma_\delta)$$

$$\lesssim \delta^4 + \delta \cdot \delta^{2+\mu} \cdot \delta^2 \cdot \delta^{-2} \approx \delta^{3+\mu}.$$

$$\square$$

Remark 2.3. Although the auxiliary solution $\widetilde{u}_0$ is required to be $C_b^4(\widehat{\Omega}_\delta)$, the nonlocal solution itself u_δ is not subject to this restriction. As we will see in Section 5.2, u_δ could be discontinuous across $\partial\Omega$.

It is worth pointing out that, nonlocal models with the second order convergence rate to the local limit in the L^∞ norm have been studied in [20, 23, 33, 38, 39]. In [42], the authors considered nonlocal integral relaxations of local differential equations on a manifold, and proved the second-order convergence in the H^1 semi-norm to the local counterpart, although the nonlocal relaxation used there is different from what we discuss in this paper.

In the rest of this paper, we take two-dimensional cases for illustration. A similar process of numerical analysis and the corresponding results can be readily extended to higher dimensions.

2.2. Convergence of the nonlocal solutions with polygonal approximations of the spherical interaction neighborhoods.

To make the analysis more concise, we assume that $\widetilde{\gamma}_\delta$ has a re-scaled form, that is,

$$(2.5) \qquad \widetilde{\gamma}_\delta(s) = \frac{1}{\delta^4} \gamma\left(\frac{s}{\delta}\right)$$

for some nonnegative function γ defined on $(0,1)$. Then by the normalization condition given in (1.4) we have

$$\int_{B_1(\mathbf{0})} \xi_i^2 \gamma\left(|\boldsymbol{\xi}|_2\right) d\boldsymbol{\xi} = 1, \ \ i = 1, 2.$$

Denote by

$$\Phi(t) = \frac{1}{2} \int_{|\boldsymbol{\xi}|_2 \leq t} |\boldsymbol{\xi}|_2^2 \cdot \gamma(|\boldsymbol{\xi}|_2) d\boldsymbol{\xi} = \pi \int_0^t \rho^3 \gamma(\rho) d\rho, \quad \Psi(t) = 4 \int_0^t \rho^2 \gamma(\rho) d\rho.$$

Thus $\Phi(1) = 1$ according to (1.4), and for $t \in (0,1]$,

$$\Phi'(t) = \pi t^3 \gamma(t), \quad \Psi'(t) = 4t^2 \gamma(t).$$
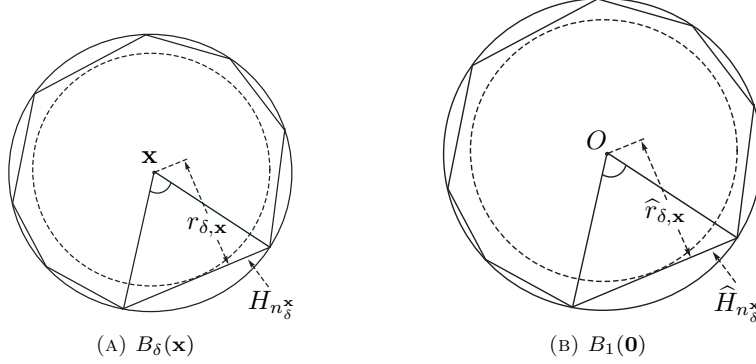

(A) $B_\delta(\mathbf{x})$ (B) $B_1(\mathbf{0})$

FIGURE 2. Inscribed polygon in $B_\delta(\mathbf{x})$ and its image by (2.6)

For any $\mathbf{x} \in \Omega$, an inscribed polygon of the circle $B_\delta(\mathbf{x})$ is denoted by $B_{\delta,n_\delta^{\mathbf{x}}}(\mathbf{x})$, or simply $B_{\delta,n_\delta^{\mathbf{x}}}$, where $n_\delta^{\mathbf{x}}$ denotes its number of sides. Furthermore, by (2.5) the rescaled polygon of $B_{\delta,n_\delta^{\mathbf{x}}}$ is defined as

$$(2.6) \qquad B_{1,n_\delta^{\mathbf{x}}}(\mathbf{0}) = \left\{ \mathbf{z} = (\mathbf{y} - \mathbf{x}) / \delta : \mathbf{y} \in B_{\delta,n_\delta^{\mathbf{x}}} \right\}.$$

For a given $\delta > 0$ and a family of polygons $\{B_{\delta,n_\delta^{\mathbf{x}}}\}_{\mathbf{x}}$, we introduce the notation

$$n_\delta = \sup_{\mathbf{x} \in \Omega} n_\delta^{\mathbf{x}}, \quad n_{\delta,\inf} = \inf_{\mathbf{x} \in \Omega} n_\delta^{\mathbf{x}}.$$

Denote by $r_{\delta,\mathbf{x}}$ the radius of the largest circle (centered on $\mathbf{x}$) contained in $B_{\delta,n_\delta^{\mathbf{x}}}$, see (A) of Figure 2, and $r(n_\delta) = \inf_{\mathbf{x} \in \Omega} r_{\delta,\mathbf{x}}$.

Let us define the weakly quasi-uniformity for a family of inscribed polygons which is weaker than the quasi-uniformity introduced in [17].

Definition 2.4. A family of inscribed polygons $\{B_{\delta,n_\delta^{\mathbf{x}}}\}$ is called weakly quasi-uniform if there exist two constants C_1 and $C_2 > 0$ such that $\forall \delta > 0$, the following two bounds hold

$$\sup_{\mathbf{x} \in \Omega} \frac{H_{n_\delta^{\mathbf{x}}}}{2 \sin (\pi/n_\delta^{\mathbf{x}})} \leq C_1 \delta, \quad \text{and} \quad \inf_{\mathbf{x} \in \Omega} r_{\delta,\mathbf{x}} \geq C_2 \delta$$

where $H_{n_\delta^{\mathbf{x}}}$ stands for the length of the longest side of $B_{\delta,n_\delta^{\mathbf{x}}}$, see (A) of Figure 2.

For a weakly quasi-uniform family of inscribed polygons, there exists a constant $C_3 > 0$ such that for all $\delta > 0$, $n_\delta \leq C_3 n_{\delta,\inf}$ holds. Denoted by

$$B'_{\delta,n_\delta^{\mathbf{x}}} = \{\mathbf{y} \in B_\delta(\mathbf{x}) : \mathbf{x} \in B_{\delta,n_\delta^{\mathbf{y}}}\},$$

then the family of kernels

$$\gamma_{\delta,n_\delta}(\mathbf{x}, \mathbf{y}) = \frac{1}{2} \gamma_\delta(\mathbf{x}, \mathbf{y}) \left(\chi_{B_{\delta,n_\delta^{\mathbf{x}}}}(\mathbf{y}) + \chi_{B'_{\delta,n_\delta^{\mathbf{x}}}}(\mathbf{y}) \right)$$

are symmetric with respect to $\mathbf{x}$ and $\mathbf{y}$, but not radial. We then define a family of nonlocal operators

$$\mathcal{L}_{\delta,n_\delta}u(\mathbf{x}) = 2 \int_{\mathbb{R}^2} \left(u(\mathbf{y}) - u(\mathbf{x})\right) \gamma_{\delta,n_\delta}(\mathbf{x},\mathbf{y})d\mathbf{y} \quad \forall \mathbf{x} \in \Omega,$$

and the corresponding family of nonlocal problems

$$(2.7) \qquad \begin{cases} -\mathcal{L}_{\delta,n_\delta}u_{\delta,n_\delta}(\mathbf{x}) &= f_\delta(\mathbf{x}) \quad \text{on } \Omega, \\ u_{\delta,n_\delta}(\mathbf{x}) &= g_\delta(\mathbf{x}) \quad \text{on } \Omega_\delta^c. \end{cases}$$

The nonlocal energy inner product associated with $-\mathcal{L}_{\delta,n_\delta}$ and the corresponding norm are defined as follows

$$(u,v)_{\delta,n_\delta} := \int_{\widehat{\Omega}_\delta} \int_{\widehat{\Omega}_\delta} \left(u(\mathbf{y}) - u(\mathbf{x})\right)\left(v(\mathbf{y}) - v(\mathbf{x})\right) \gamma_{\delta,n_\delta}(\mathbf{x},\mathbf{y})d\mathbf{y}d\mathbf{x},$$

$$\|u\|_{\delta,n_\delta} := (u,u)_{\delta,n_\delta}^{1/2}.$$

To simplify the notation, let $\|u\|_{r(n_\delta)}$ be the same as $\|\cdot\|_\delta$ except for the replacement of δ by $r(n_\delta)$. As derived in [17] we have

$$(2.8) \qquad \|u\|_{r(n_\delta)} \leq \|u\|_{\delta,n_\delta} \leq \|u\|_\delta.$$

It is worth noting that for a fixed point $\mathbf{x}$, the support of $\gamma_{\delta,n_\delta}(\mathbf{x},\mathbf{y})$ is not necessarily symmetric, so the integral of $(\mathbf{y} - \mathbf{x})\gamma_{\delta,n_\delta}(\mathbf{x},\mathbf{y})$ does not necessarily vanish. In order to inherit the symmetric-support property of the original kernel γ_δ, we define kernels

$$\gamma_{\delta|n_\delta}(\mathbf{x},\mathbf{y}) = \frac{1}{2}\gamma_\delta(\mathbf{x},\mathbf{y}) \left(\chi_{B_{\delta,n_\delta^\times}}(\mathbf{y}) + \chi_{B_{\delta,n_\delta^\times}^T}(\mathbf{y})\right),$$

with

$$B_{\delta,n_\delta^\times}^T = \{\mathbf{y} \in B_\delta(\mathbf{x}) : 2\mathbf{x} - \mathbf{y} \in B_{\delta,n_\delta^\times}\}.$$

Based on the definition of $\gamma_{\delta|n_\delta}$, we define a new family of nonlocal operators

$$\mathcal{L}_{\delta|n_\delta}u(\mathbf{x}) = 2 \int_{\mathbb{R}^2} \left(u(\mathbf{y}) - u(\mathbf{x})\right) \gamma_{\delta|n_\delta}(\mathbf{x},\mathbf{y})d\mathbf{y} \quad \forall \mathbf{x} \in \Omega,$$

and the corresponding family of nonlocal problems

$$(2.9) \qquad \begin{cases} -\mathcal{L}_{\delta|n_\delta}u_{\delta|n_\delta}(\mathbf{x}) &= f_\delta(\mathbf{x}) \quad \text{on } \Omega, \\ u_{\delta|n_\delta}(\mathbf{x}) &= g_\delta(\mathbf{x}) \quad \text{on } \Omega_\delta^c, \end{cases}$$

where the support of the kernel is a symmetric polygon for any fixed point $\mathbf{x}$. However, the operator $-\mathcal{L}_{\delta|n_\delta}$ is not self-adjoint/symmetric so we could not directly define the corresponding inner product and norm.

We recall [17] to show that neither $\mathcal{L}_{\delta,n_\delta}\left(|\mathbf{x}|_2^2\right)$ nor $\mathcal{L}_{\delta|n_\delta}\left(|\mathbf{x}|_2^2\right)$ converges to $\mathcal{L}_0\left(|\mathbf{x}|_2^2\right)$ if n_δ is uniformly bounded, as $\delta \to 0$.

Theorem 2.5. [17, Theorem 3.1] *Assume* $\left\{B_{\delta,n_\delta^\times}\right\}$ *is a family of polygons which satisfies* $B_{\delta,n_\delta^\times} \subset B_\delta(\mathbf{x})$, $\forall \delta$, $\forall \mathbf{x} \in \Omega$. *The family of kernels* $\{\gamma_\delta\}$ *satisfies the conditions* (1.3) *and* (1.4). *If* n_δ *is uniformly bounded as* $\delta \to 0$, *then both* $\mathcal{L}_{\delta,n_\delta}\left(|\mathbf{x}|_2^2\right)$ *and* $\mathcal{L}_{\delta|n_\delta}\left(|\mathbf{x}|_2^2\right)$ *do not converge to* $\mathcal{L}_0\left(|\mathbf{x}|_2^2\right)$ *for all* $\mathbf{x} \in \Omega$.

Next, we want to establish the error estimate between $u_{\delta|n_\delta}$ and $\widetilde{u}_0$. To do that, we need a theorem of the maximum-principle type, which is important for the derivation of the estimate of $u_{\delta|n_\delta} - \widetilde{u}_0$, once the estimate for $-\mathcal{L}_{\delta|n_\delta}\left(u_{\delta|n_\delta} - \widetilde{u}_0\right)$ is available.

Theorem 2.6. *Assume that γ_δ satisfies (1.3) and the first two of (1.4). If $f_\delta(\mathbf{x}) \leq 0$, for all $\mathbf{x} \in \Omega$, then*

$$(2.10) \qquad \sup_{\mathbf{x}\in\Omega} u_{\delta|n_\delta}(\mathbf{x}) \leq \sup_{\mathbf{x}\in\Omega_\delta^c} g_\delta(\mathbf{x}).$$

Proof. Set $M = \sup_{\mathbf{x}\in\Omega} u_{\delta|n_\delta}(\mathbf{x})$. We begin with the following case:

$$(2.11) \qquad f_\delta(\mathbf{x}) \leq -\eta < 0,\ \forall \mathbf{x} \in \Omega,$$

where η is an arbitrary positive number. In this case we prove (2.10) by contradiction. If (2.10) does not hold. By the definition of M, we know that $u_{\delta|n_\delta}(\mathbf{y}) \leq M$, $\forall \mathbf{y} \in \Omega$ and there exists a point $\mathbf{x}_0 \in \Omega$ such that $u_{\delta|n_\delta}(\mathbf{x}_0) > M - \eta/4/G(\gamma_\delta)$. Then

$$f_\delta(\mathbf{x}_0) = -\mathcal{L}_{\delta|n_\delta} u_{\delta|n_\delta}(\mathbf{x}_0) = 2\int_{B_\delta(\mathbf{x}_0)} \left(u_{\delta|n_\delta}(\mathbf{x}_0) - u_{\delta|n_\delta}(\mathbf{y})\right)\gamma_{\delta|n_\delta}(\mathbf{x}_0,\mathbf{y})d\mathbf{y}$$

$$> 2\int_{B_\delta(\mathbf{x}_0)} \left(M - u_{\delta|n_\delta}(\mathbf{y})\right)\gamma_{\delta|n_\delta}(\mathbf{x}_0,\mathbf{y})d\mathbf{y} - 2\cdot\frac{\eta}{4G(\gamma_\delta)}\cdot G(\gamma_\delta) \geq -\eta/2,$$

which contradicts (2.11).

For the general case, i.e. $f_\delta(\mathbf{x}) \leq 0$ for all $\mathbf{x} \in \Omega$, we introduce the notation

$$\widehat{r}_{\delta,\mathbf{x}} = r_{\delta,\mathbf{x}}/\delta,\ \ \widehat{H}_{n_\delta^{\mathbf{x}}} = H_{n_\delta^{\mathbf{x}}}/\delta,\ \ \hat{r}(n_\delta) = r(n_\delta)/\delta,\ \ \hat{r} = \inf_\delta\{\hat{r}(n_\delta)\},\ \ \eta^* = 4\Phi(\hat{r}).$$

One can see (B) of Figure 2 for the description of $\widehat{r}_{\delta,\mathbf{x}}$ and $\widehat{H}_{n_\delta^{\mathbf{x}}}$. Since Ω is bounded, there exists a point $\mathbf{x}^* \in \Omega$ and a constant R such that $\widehat{\Omega}_\delta \subset B_R(\mathbf{x}^*)$. Set $q(\mathbf{x}) = |\mathbf{x} - \mathbf{x}^*|_2^2$, then for all $\mathbf{x} \in \Omega$, it holds that

$$\mathcal{L}_{\delta|n_\delta} q(\mathbf{x}) = 2\int_{B_\delta(\mathbf{x})} \left(q(\mathbf{y}) - q(\mathbf{x})\right)\gamma_{\delta|n_\delta}(\mathbf{x},\mathbf{y})d\mathbf{y}$$

$$= 2\int_{B_\delta(\mathbf{x})} |\mathbf{y} - \mathbf{x}|_2^2 \gamma_{\delta|n_\delta}(\mathbf{x},\mathbf{y})d\mathbf{y} + 4\left(\mathbf{x} - \mathbf{x}^*\right)\cdot \underbrace{\int_{B_\delta(\mathbf{x})} (\mathbf{y} - \mathbf{x})\gamma_{\delta|n_\delta}(\mathbf{x},\mathbf{y})d\mathbf{y}}_{=\mathbf{0}}$$

$$(2.12)\qquad \geq 2\int_{B_{r(n_\delta)}(\mathbf{x})} |\mathbf{y} - \mathbf{x}|_2^2 \cdot \gamma_\delta(\mathbf{x},\mathbf{y})d\mathbf{y} \geq \eta^*.$$

With an arbitrary $\varepsilon > 0$, $u_{\delta|n_\delta} + \varepsilon q$ is the solution of the following problem:

$$\begin{cases} -\mathcal{L}_{\delta|n_\delta} v(\mathbf{x}) &= f_\delta(\mathbf{x}) - \varepsilon\mathcal{L}_{\delta|n_\delta} q(\mathbf{x}), & \text{on } \Omega, \\ v(\mathbf{x}) &= g_\delta(\mathbf{x}) + \varepsilon q(\mathbf{x}), & \text{on } \Omega_\delta^c. \end{cases}$$

Since $f_\delta(\mathbf{x}) - \varepsilon\mathcal{L}_{\delta|n_\delta} q(\mathbf{x}) \leq -\varepsilon\eta^* < 0$, by the previous argument, we have

$$\sup_{\mathbf{x}\in\Omega}(u_{\delta|n_\delta}(\mathbf{x}) + \varepsilon q(\mathbf{x})) \leq \sup_{\mathbf{x}\in\Omega_\delta^c}(g_\delta(\mathbf{x}) + \varepsilon q(\mathbf{x})).$$

Sending ε to zero, we complete the proof. $\qquad\square$

Theorem 2.7. *Assume that γ_δ satisfies (1.3) and the first two of (1.4). It holds*

$$\|u\|_{C(\Omega)} \leq \|u\|_{C(\Omega_\delta^c)} + C_4 \left\|\mathcal{L}_{\delta|n_\delta} u\right\|_{C(\Omega)},$$

with

$$C_4 = \frac{2\|q\|_{C(\Omega_\delta^c)}}{\eta^*} \leq \frac{R^2}{2\Phi(\hat{r})}.$$

Proof. Set for $\mathbf{x} \in \Omega$ that

$$v^\pm(\mathbf{x}) = \pm u(\mathbf{x}) - \left\|\mathcal{L}_{\delta|n_\delta} u\right\|_{C(\Omega)} \cdot q(\mathbf{x})/\eta^*.$$

By (2.12) we have

$$\mathcal{L}_{\delta|n_\delta} v^\pm(\mathbf{x}) = \pm\mathcal{L}_{\delta|n_\delta} u(\mathbf{x}) - \left\|\mathcal{L}_{\delta|n_\delta} u\right\|_{C(\Omega)} \cdot \mathcal{L}_{\delta|n_\delta} q(\mathbf{x})/\eta^* \leq 0, \ \ \mathbf{x} \in \Omega.$$

Applying Theorem 2.6, we obtain

$$\left\|v^\pm\right\|_{C(\Omega)} \leq \|u\|_{C(\Omega_\delta^c)} + \left\|\mathcal{L}_{\delta|n_\delta} u\right\|_{C(\Omega)} \|q\|_{C(\Omega_\delta^c)}/\eta^*.$$

Thus we complete the proof. $\qquad\square$

Theorem 2.8. *Suppose conditions of Theorem 2.2 hold, $\left\{B_{\delta,n_\delta^\times}\right\}$ is a weakly quasi-uniform family of inscribed polygons. Let $u_{\delta|n_\delta}$ be the solution of the nonlocal problem (2.9). If $n_\delta \to \infty$ as $\delta \to 0$, then it holds that*

$$(2.13) \qquad \left\|u_{\delta|n_\delta} - u_0\right\|_{C(\Omega)} = O\left(\delta^2\right) + O\left(n_\delta^{-\lambda}\right),$$

$$(2.14) \qquad \left\|u_{\delta|n_\delta} - \widetilde{u}_0\right\|_\delta = O\left(\delta^{(3+\mu)/2}\right) + O\left(n_\delta^{-\lambda}\right),$$

with

$$(2.15) \qquad \lambda = \begin{cases} 2, & \text{if } \Phi'(1) \neq 0, \\ 4, & \text{if } \Phi'(1) = 0, \ \Phi''(1) \neq 0. \end{cases}$$

Proof. Since $\widetilde{u}_0 \in C_b^4(\widehat{\Omega}_\delta)$, a direct calculation leads to

$$(2.16) \qquad \mathcal{L}_{\delta|n_\delta}\widetilde{u}_0(\mathbf{x}) = \sum_{i=1}^2 \sigma_{n_\delta}^i(\mathbf{x})\partial_{ii}\widetilde{u}_0(\mathbf{x}) + O\left(\delta^2\right)|\widetilde{u}_0|_{4,\infty,\widehat{\Omega}_\delta}$$

with (the notation is slightly different from that in [17])

$$\sigma_{n_\delta}^i(\mathbf{x}) = \int_{B_\delta(\mathbf{x})} (y_i - x_i)^2 \gamma_{\delta|n_\delta}(\mathbf{x},\mathbf{y}) d\mathbf{y}, \ i = 1, 2.$$

By the definition of $r(n_\delta)$, we know for all $\mathbf{x} \in \Omega$ that

$$(2.17) \qquad \int_{|\mathbf{z}|_2 < r(n_\delta)} z_i^2 \widetilde{\gamma}_\delta\left(|\mathbf{z}|_2\right) d\mathbf{z} \leq \sigma_{n_\delta}^i(\mathbf{x}) \leq \int_{|\mathbf{z}|_2 < \delta} z_i^2 \widetilde{\gamma}_\delta\left(|\mathbf{z}|_2\right) d\mathbf{z} = \Phi(1) = 1,$$

where

$$\int_{|\mathbf{z}|_2 < r(n_\delta)} z_i^2 \widetilde{\gamma}_\delta\left(|\mathbf{z}|_2\right) d\mathbf{z} = \int_{|\boldsymbol{\xi}|_2 < \hat{r}(n_\delta)} \xi_i^2 \gamma\left(|\boldsymbol{\xi}|_2\right) d\boldsymbol{\xi} = \Phi\left(\hat{r}(n_\delta)\right).$$

By weak quasi-uniformity of the inscribed polygons, we have for any $\mathbf{x} \in \Omega$,

$$\hat{r}_{\delta,\mathbf{x}}^2 = 1 - \left(\widehat{H}_{n_\delta^\times}/2\right)^2 \geq 1 - C_1^2 \sin^2\left(\pi/n_\delta^\times\right) \geq 1 - C_1^2 \sin^2\left(\pi/n_{\delta,\inf}\right)$$

$$\geq 1 - C_1^2 \sin^2\left(C_3\pi/n_\delta\right).$$

Taking the infimum on both sides of the above inequality, we have

$$\hat{r}(n_\delta)^2 \geq 1 - C_1^2 \sin^2\left(C_3\pi/n_\delta\right),$$

which leads to

$$1 - \hat{r}(n_\delta) \leq 1 - \sqrt{1 - C_1^2 \sin^2\left(C_3\pi/n_\delta\right)} = C_1^2 C_3^2 \pi^2/2/n_\delta^2 + O\left(n_\delta^{-4}\right).$$

By the Taylor expansion of $\Phi(t)$ at the point $t = 1$,

$$1 - \int_{|\mathbf{z}|_2 < r(n_\delta)} z_i^2 \widetilde{\gamma}_\delta\left(|\mathbf{z}|_2\right) d\mathbf{z} = \Phi(1) - \Phi\left(\hat{r}(n_\delta)\right)$$

$$= \begin{cases} \Phi'(1)\left(1 - \hat{r}(n_\delta)\right) + o\left(1 - \hat{r}(n_\delta)\right) & = O\left(n_\delta^{-2}\right), \text{ if } \Phi'(1) \neq 0, \\ -\Phi''(1)\frac{(1-\hat{r}(n_\delta))^2}{2} + o\left((1 - \hat{r}(n_\delta))^2\right) & = O\left(n_\delta^{-4}\right), \text{ if } \Phi'(1) = 0,\ \Phi''(1) \neq 0. \end{cases}$$

Thus, by (2.15) and (2.17) we have

$$(2.18) \qquad 1 - \sigma_{n_\delta}^i(\mathbf{x}) \leq 1 - \int_{|\mathbf{z}|_2 < r(n_\delta)} z_i^2 \widetilde{\gamma}_\delta\left(|\mathbf{z}|_2\right) d\mathbf{z} = O\left(n_\delta^{-\lambda}\right).$$

Together with (2.16) and (2.2) it holds that

$$(2.19) \qquad \begin{cases} -\mathcal{L}_{\delta|n_\delta}\left(u_{\delta|n_\delta} - \widetilde{u}_0\right)(\mathbf{x}) = O\left(\delta^2\right) + O\left(n_\delta^{-\lambda}\right), & \mathbf{x} \in \Omega, \\ u_{\delta|n_\delta}(\mathbf{x}) - \widetilde{u}_0(\mathbf{x}) = g_\delta(\mathbf{x}) - \widetilde{u}_0(\mathbf{x}) = O\left(\delta^{2+\mu}\right), & \mathbf{x} \in \Omega_\delta^c. \end{cases}$$

A direct application of the maximum principle Theorem 2.7 to (2.19) produces

$$\left\|u_{\delta|n_\delta} - u_0\right\|_{C(\Omega)} = O\left(\delta^2\right) + O\left(n_\delta^{-\lambda}\right)$$

This is (2.13), which, together with (2.1) and (2.19), leads to

$$\left\|u_{\delta|n_\delta} - \widetilde{u}_0\right\|_\delta^2 = -\int_\Omega \left(u_{\delta|n_\delta}(\mathbf{x}) - u_0(\mathbf{x})\right) \mathcal{L}_\delta\left(u_{\delta|n_\delta} - \widetilde{u}_0\right)(\mathbf{x}) d\mathbf{x}$$

$$- \int_{\Omega_\delta^c} \left(g_\delta(\mathbf{x}) - \widetilde{u}_0(\mathbf{x})\right) \int_{\widehat{\Omega}_\delta} \left(u_{\delta|n_\delta}(\mathbf{y}) - \widetilde{u}_0(\mathbf{y}) - g_\delta(\mathbf{x}) + \widetilde{u}_0(\mathbf{x})\right) \gamma_\delta(\mathbf{x}, \mathbf{y}) d\mathbf{y} d\mathbf{x}$$

$$\lesssim \left(\delta^2 + n_\delta^{-\lambda}\right)^2 + |\Omega_\delta^c| \cdot \|g_\delta - \widetilde{u}_0\|_{C(\Omega_\delta^c)} \left(\left\|u_{\delta|n_\delta} - u_0\right\|_{C(\Omega)} + \|g_\delta - \widetilde{u}_0\|_{C(\Omega_\delta^c)}\right) G(\gamma_\delta)$$

$$\lesssim \left(\delta^2 + n_\delta^{-\lambda} + \delta^{-1}\|g_\delta - \widetilde{u}_0\|_{C(\Omega_\delta^c)}\right)\left(\delta^2 + n_\delta^{-\lambda}\right).$$

Together with (2.2), we get (2.14). The proof is complete.   □

By Theorem 2.8, if $n_\delta \to \infty$ as $\delta \to 0$, then $\{u_{\delta|n_\delta}\}$ converges to $\widetilde{u}_0$ in $\|\cdot\|_{C(\Omega)}$ (thus in $\|\cdot\|_{L^2(\Omega)}$) and $\|\cdot\|_\delta$ norms. This offers a contrast with the conclusion of Theorem 2.5.

Similar to Theorem 2.8, the error estimate for the nonlocal solutions with non-symmetric polygonal interaction neighborhoods against their local counterpart can be established. To state the result, we first introduce some notations. Let

$$\sigma_{n_\delta}^{i,1}(\mathbf{x}) = \int_{\widehat{\Omega}_\delta} (y_i - x_i)\gamma_{\delta,n_\delta}(\mathbf{x}, \mathbf{y}) d\mathbf{y},$$

$$\sigma_{n_\delta}^{ij,2}(\mathbf{x}) = \int_{\widehat{\Omega}_\delta} (y_i - x_i)(y_j - x_j)\gamma_{\delta,n_\delta}(\mathbf{x}, \mathbf{y}) d\mathbf{y},$$

$$\sigma_{n_\delta}^{\boldsymbol{\alpha},3}(\mathbf{x}) = \frac{1}{\boldsymbol{\alpha}!}\int_{\widehat{\Omega}_\delta} (y_1 - x_1)^{\alpha_1}(y_2 - x_2)^{\alpha_2}\gamma_{\delta,n_\delta}(\mathbf{x}, \mathbf{y}) d\mathbf{y}.$$

Theorem 2.9. *Suppose the conditions of Theorem 2.8 hold. Let u_{δ,n_δ} be the solution of the nonlocal problem (2.7). Under the condition*

$$\left|\sigma_{n_\delta}^{i,1}(\mathbf{x})\right| \to 0, \;\; i = 1, 2, \;\; as \; \delta \to 0, \tag{2.20}$$

it holds that

$$\|u_{\delta,n_\delta} - u_0\|_{C(\Omega)} = O\left(\delta^2\right) + O\left(\delta^{-1}n_\delta^{-\lambda}\right), \tag{2.21}$$

$$\|u_{\delta,n_\delta} - \widetilde{u}_0\|_{\delta,n_\delta} = O\left(\delta^{(3+\mu)/2}\right) + O\left(\delta^{-1}n_\delta^{-\lambda}\right). \tag{2.22}$$

Proof. A direct calculation shows that

$$\mathcal{L}_{\delta,n_\delta}\widetilde{u}_0(\mathbf{x}) = F(\mathbf{x}) + \sum_{i=1}^{2}\sigma_{n_\delta}^{ii,2}(\mathbf{x})\partial_{ii}\widetilde{u}_0(\mathbf{x}) + O\left(\delta^2\right),$$

where

$$F(\mathbf{x}) = 2\sum_{i=1}^{2}\sigma_{n_\delta}^{i,1}(\mathbf{x})\partial_i\widetilde{u}_0(\mathbf{x}) + 2\sigma_{n_\delta}^{12,2}(\mathbf{x})\partial_{12}\widetilde{u}_0(\mathbf{x}) + 2\sum_{|\boldsymbol{\alpha}|=3}\sigma_{n_\delta}^{\boldsymbol{\alpha},3}(\mathbf{x})\partial_{\boldsymbol{\alpha}}\widetilde{u}_0(\mathbf{x}).$$

Similar to the proof of (2.18), we have $1 - \sigma_{n_\delta}^{ii,2}(\mathbf{x}) = O\left(n_\delta^{-\lambda}\right)$. Thus, it holds that

$$\begin{cases} -\mathcal{L}_{\delta,n_\delta}\left(u_{\delta,n_\delta} - \widetilde{u}_0\right)(\mathbf{x}) = O\left(\delta^2\right) + O\left(n_\delta^{-\lambda}\right) + F(\mathbf{x}), & \mathbf{x} \in \Omega, \\ u_{\delta,n_\delta}(\mathbf{x}) - \widetilde{u}_0(\mathbf{x}) = g_\delta(\mathbf{x}) - \widetilde{u}_0(\mathbf{x}) = O\left(\delta^{2+\mu}\right), & \mathbf{x} \in \Omega_\delta^c. \end{cases} \tag{2.23}$$

A direct application of nonlocal maximum principle similar to Theorems 2.6 and 2.7 (but with the condition (2.20)) to (2.23) produces

$$\|u_{\delta,n_\delta} - u_0\|_{C(\Omega)} = O\left(\delta^2\right) + O\left(n_\delta^{-\lambda}\right) + F_s, \tag{2.24}$$

where $F_s = \sup_{\mathbf{x}\in\Omega}|F(\mathbf{x})|$. By the definition of γ_{δ,n_δ}, we have

$$2\sigma_{n_\delta}^{i,1}(\mathbf{x}) = 2\int_{B_\delta(\mathbf{x})}(y_i - x_i)\gamma_{\delta,n_\delta}(\mathbf{x},\mathbf{y})d\mathbf{y}$$

$$= 2\underbrace{\int_{B_\delta(\mathbf{x})}(y_i - x_i)\gamma_\delta(\mathbf{x},\mathbf{y})d\mathbf{y}}_{=0} - \left(\int_{B_\delta(\mathbf{x})\backslash B_{\delta,n_\delta^{\mathbf{x}}}} + \int_{B_\delta(\mathbf{x})\backslash B'_{\delta,n_\delta^{\mathbf{x}}}}\right)(y_i - x_i)\gamma_\delta(\mathbf{x},\mathbf{y})d\mathbf{y}.$$

Thus the following estimate holds

$$\left|\sigma_{n_\delta}^{i,1}(\mathbf{x})\right| \leq \frac{1}{2}\int_{B_\delta(\mathbf{x})\backslash B_{\delta,n_\delta^{\mathbf{x}}}} + \int_{B_\delta(\mathbf{x})\backslash B'_{\delta,n_\delta^{\mathbf{x}}}} |y_i - x_i|\,\gamma_\delta(\mathbf{x},\mathbf{y})d\mathbf{y}$$

$$\leq \int_{|\mathbf{z}|_2 < \delta}|z_i|\widetilde{\gamma}_\delta\left(|\mathbf{z}|_2\right)d\mathbf{z} - \int_{|\mathbf{z}|_2 < r(n_\delta)}|z_i|\widetilde{\gamma}_\delta\left(|\mathbf{z}|_2\right)d\mathbf{z}$$

$$= \delta^{-1}\left[\Psi(1) - \Psi(\hat{r}(n_\delta))\right] = O\left(\delta^{-1}n_\delta^{-\lambda}\right),$$

where we use the Taylor expansion of $\Psi(t)$ at point $t = 1$. Similarly,

$$\left|\sigma_{n_\delta}^{12,2}(\mathbf{x})\right| = O\left(n_\delta^{-\lambda}\right), \;\; \left|\sigma_{n_\delta}^{\boldsymbol{\alpha},3}(\mathbf{x})\right| = O\left(\delta n_\delta^{-\lambda}\right).$$

Then $F_s = O\left(\delta^{-1} n_\delta^{-\lambda}\right)$. Inserting this into (2.24), we get (2.21) which, together with (2.23) and (2.1), leads to

$$\|u_{\delta,n_\delta} - \widetilde{u}_0\|^2_{\delta,n_\delta} \lesssim \left(\delta^2 + n_\delta^{-\lambda} + F_s\right)^2 + |\Omega_\delta^c| \cdot \|g_\delta - \widetilde{u}_0\|_{C(\Omega_\delta^c)} \left(\delta^2 + n_\delta^{-\lambda} + F_s\right) G(\gamma_\delta)$$

$$\lesssim \left(\delta^2 + n_\delta^{-\lambda} + F_s\right) \cdot \left(\delta^{1+\mu} + n_\delta^{-\lambda} + F_s\right).$$

Thus, using the bound of F_s, we complete the proof. $\square$

From Theorem 2.9, we know that even when $n_\delta \to \infty$, $\{u_{\delta,n_\delta}\}$ might not converge to $\widetilde{u}_0$ in $\|\cdot\|_{C(\Omega)}$ or $\|\cdot\|_{\delta,n_\delta}$ as $\delta \to 0$. The reason is that the support of $\gamma_{\delta,n_\delta}(\mathbf{x}, \mathbf{y})$ is not symmetric with respect to $\mathbf{x}$, so the integral of the product of the kernel with an odd function does not necessarily vanish. On the other hand, we could only prove the nonlocal maximum principle with the condition (2.20). Thus, an additional condition is required to ensure the convergence in $\|\cdot\|_{C(\Omega)}$ or $\|\cdot\|_{\delta,n_\delta}$: $F_s \to 0$ as $\delta \to 0$. However, one may observe the convergence in the L^2 norm numerically even without this condition, see numerical results in Section 5 and additional discussions in Remark 3.4.

We could also prove lower bounds for $1 - \sigma^i_{n_\delta}(\mathbf{x})$ and $1 - \sigma^{i,1}_{n_\delta}(\mathbf{x})$ which play a helpful role in assessing whether the nonlocal operators converge to the local operator. The next theorem provides a lower bound for $1 - \sigma^i_{n_\delta}(\mathbf{x})$.

Theorem 2.10. *Suppose the family $\{\gamma_\delta\}$ satisfies (1.3) and (1.4), while $\{B_{\delta,n_\delta^\times}\}$ is a family of inscribed polygons. If $n_\delta \leq N$ for all δ, then we have for $\Phi'(1) \neq 0$,*

$$(2.25) \qquad\qquad 1 - \sigma^i_{n_\delta}(\mathbf{x}) \geq L_1 \cdot \sigma_{L,1}(\pi/N)/\pi,$$

with

$$L_1 = \min_{\cos(\pi/N) \leq t \leq 1} \Phi'(t), \ \ \sigma_{L,1}(s) = \frac{s}{2} + \frac{1}{4}\sin(2s) - \cos(s)\log\left(\tan\left(\frac{s}{2} + \frac{\pi}{4}\right)\right),$$

and for $\Phi'(1) = 0$, $\Phi''(1) \neq 0$,

$$(2.26) \qquad\qquad 1 - \sigma^i_{n_\delta}(\mathbf{x}) \geq L_2 \cdot \sigma_{L,2}(\pi/N)/\pi,$$

with

$$L_2 = \min_{\cos(\pi/N) \leq t \leq 1} |\Phi''(t)|, \sigma_{L,2}(s) = \frac{5}{8}\sin(2s) - \frac{s}{4}\cos(2s) - \cos(s)\log\left(\tan\left(\frac{s}{2} + \frac{\pi}{4}\right)\right).$$

Proof. Consider the section of the longest side in $B_{1,n_\delta^\times}(\mathbf{0})$, which is composed of a triangle and its adjoining cap. Denote the cap by $C_{n_\delta^\times}$, then $C_{n_\delta^\times} \subset B_1(\mathbf{0}) \backslash B_{1,n_\delta^\times}(\mathbf{0})$, and

$$2\left(1 - \sigma^i_{n_\delta}(\mathbf{x})\right) = 2\int_{B_\delta(\mathbf{x})} (y_i - x_i)^2 \gamma_\delta(\mathbf{x}, \mathbf{y})d\mathbf{y} - 2\int_{B_\delta(\mathbf{x})} (y_i - x_i)^2 \gamma_{\delta|n_\delta}(\mathbf{x}, \mathbf{y})d\mathbf{y}$$

$$= \int_{B_\delta(\mathbf{x})} (y_i - x_i)^2 \gamma_\delta(\mathbf{x}, \mathbf{y})\left(1 - \chi_{B_{\delta,n_\delta^\times}}(\mathbf{y}) + 1 - \chi_{B^T_{\delta,n_\delta^\times}}(\mathbf{y})\right)d\mathbf{y}$$

$$\geq \int_{B_\delta(\mathbf{x})} (y_i - x_i)^2 \gamma_\delta(\mathbf{x}, \mathbf{y})\left(1 - \chi_{B_{\delta,n_\delta^\times}}(\mathbf{y})\right)d\mathbf{y} \geq \int_{C_{n_\delta^\times}} \xi_i^2 \gamma\left(\|\boldsymbol{\xi}\|_2\right)d\boldsymbol{\xi}.$$

According to different orientations, the value of

$$\frac{1}{2}\int_{C_{n_\delta^\times}} \xi_i^2 \gamma\left(\|\boldsymbol{\xi}\|_2\right)d\boldsymbol{\xi}$$

may differ. However, we can estimate a lower bound for all cases. For $\Phi'(1) \neq 0$,

$$\frac{1}{2} \int_{C_{n_\delta^\mathbf{x}}} \xi_i^2 \gamma \left(\|\boldsymbol{\xi}\|_2 \right) d\boldsymbol{\xi} \geq \int_0^{\frac{\pi}{N}} \sin^2(\theta) \int_{\frac{\cos(\pi/N)}{\cos(\theta)}}^1 \rho^3 \gamma(\rho) d\rho d\theta$$

$$= \frac{1}{\pi} \int_0^{\frac{\pi}{N}} \sin^2(\theta) \left[\Phi(1) - \Phi \left(\frac{\cos(\pi/N)}{\cos(\theta)} \right) \right] d\theta \geq \frac{L_1}{\pi} \int_0^{\frac{\pi}{N}} \sin^2(\theta) \left[1 - \frac{\cos(\pi/N)}{\cos(\theta)} \right] d\theta$$

$$= L_1 \cdot \left[\frac{\pi}{2N} + \frac{1}{4} \sin \left(\frac{2\pi}{N} \right) - \cos \left(\frac{\pi}{N} \right) \log \left(\tan \left(\frac{\pi}{2N} + \frac{\pi}{4} \right) \right) \right] / \pi,$$

which is (2.25). Using the similar argument and notice that for $\Phi'(1) = 0$, $\Phi''(1) \neq 0$

$$\Phi(1) - \Phi \left(\frac{\cos(\pi/n_\delta)}{\cos(\theta)} \right) \geq \frac{L_2}{2} \left[1 - \frac{\cos(\pi/n_\delta)}{\cos(\theta)} \right]^2,$$

then (2.26) is gotten. Thus, we complete the proof. $\qquad\square$

Note that this estimate for the lower bound of $1 - \sigma_{n_\delta}^i(\mathbf{x})$ in Theorem 2.10 might not be sharp in some cases. However, it could still play a helpful role in assessing whether the nonlocal operators converge to the local operator.

Theorem 2.10 offers a quantitative characterization of the lack of convergence stated in the Theorem 2.5. In fact, it indicates that if n_δ is uniformly bounded as $\delta \to 0$, then $\{u_{\delta|n_\delta}\}$ may converge to $\widetilde{u}_0$ only for the case of a trivial solution.

Similar results for $1 - \sigma_{n_\delta}^{i,1}(\mathbf{x})$ could be provided in the same manner, we omit that to save space for the paper.

2.3. **Examples of the kernel function.** Here we list some popular kernels in general d-dimensional setting under the assumption that $\widetilde{\gamma}_\delta$ has a re-scaled form (2.5) while replacing δ^4 (for $d = 2$) by δ^{d+2}. For more discussions on the effects of the kernels on the nonlocal models, we refer to [12, 29].

Type 1. Constant kernel:

$$(2.27) \qquad\qquad \gamma(\rho) = \frac{d(d+2)}{w_d}, \ \ 0 \leq \rho \leq 1.$$

Type 2. Linear kernel:

$$\gamma(\rho) = \frac{d(d+2)(d+3)}{w_d}(1 - \rho), \ \ 0 \leq \rho \leq 1.$$

Type 3. Gaussian-like kernel:

$$\gamma(\rho) = \frac{d}{C_e w_d} e^{-\rho^2}, \ \ 0 \leq \rho \leq 1, \ \ \text{with } C_e = \int_0^1 \tau^{d+1} e^{-\tau^2} d\tau.$$

Type 4. Peridynamic kernel [31] for $d \geq 2$:

$$\gamma(\rho) = \frac{d(d+1)}{w_d} \rho^{-1}, \ \ 0 < \rho \leq 1.$$

All four types of kernels shown above satisfy (1.3), (1.4) and (2.1). The functions $\Phi(t)$ and $\Psi(t)$ corresponding to the linear kernel (*Type* 2) satisfy the condition

$$\Phi'(1) = 0, \ \ \Psi'(1) = 0, \ \ \Phi''(1) \neq 0, \ \ \Psi'(1) \neq 0,$$

hence $\lambda = 4$. The other three types of kernels satisfy

$$\Phi'(1) \neq 0, \ \ \Psi'(1) \neq 0,$$

which leads to $\lambda = 2$.

Note that our discussion so far involves only approximations of nonlocal opera-
tors on the continuum level and we have not incorporated the effect of finite dimen-
sional discretizations of the operators. Next, we take the conforming DG (CDG)
method as a representative setting to study the discretization error. Extensions to
other types of numerical methods can be worked out analogously.

3. ERROR ESTIMATE OF THE LINEAR CDG METHOD FOR THE NONLOCAL PROBLEMS WITH RESPECT TO THE HORIZON PARAMETER AND THE MESH SIZE

In this section, we review the linear CDG method proposed in [19] for solving
nonlocal problems with integrable kernels. We then study the corresponding dis-
cretization error with respect to the horizon parameter and the mesh size. Note that
in [11] (where the continuous piecewise linear FEM is used) and [19], the analysis
is only concerned with the dependence on the mesh size.

3.1. Brief review of the linear CDG method for nonlocal problems. Now
we briefly recall the basic steps of the linear CDG method for solving the nonlo-
cal problems (1.2) to make the discussion reasonably self-contained. Firstly, the
variational form of (1.2) finds $u_\delta \in V(\widehat{\Omega}_\delta)$ such that

$$(3.1) \qquad -\int_\Omega w(\mathbf{x})\mathcal{L}_\delta u_\delta(\mathbf{x})d\mathbf{x} = \int_\Omega f_\delta(\mathbf{x})w(\mathbf{x})d\mathbf{x}, \ \forall w \in V^0(\widehat{\Omega}_\delta).$$

For a given triangulation $\mathcal{T}_\delta^h$ of $\widehat{\Omega}_\delta$ that simultaneously triangulates Ω (we call
such a triangulation consistent), let

$$\Omega_\delta^h = \mathcal{T}_\delta^h \cap \overline{\Omega}, \ \ \Omega_\delta^{c,h} = \mathcal{T}_\delta^h \cap \overline{\Omega_\delta^c}.$$

Assume that for any fixed δ, $\mathcal{T}_\delta^h$ is quasi-uniform [8] with respect to the mesh size
h. The set of inner and boundary nodes of Ω_δ^h are denoted by

$$NI = \{\mathbf{x}_j : j = 1, \cdots, n_1\}, \ \text{and} \ NB = \{\mathbf{x}_{n_1+j} : j = 1, \cdots, n_2\},$$

respectively. The set of all nodes in $\Omega_\delta^{c,h}$ is denoted by

$$NC = \{\mathbf{x}_{n_1+j} : j = 1, \cdots, n_2 + p\}.$$

Note that $NB \subset NC$. The continuous linear basis functions defined on $\mathcal{T}_\delta^h$ are
denoted by

$$\phi_j(\mathbf{x}), \ j = 1, 2, \cdots, n_1 + n_2 + p.$$

The basis functions of $V_\delta^{0,h}$ which contains all piecewise linear functions vanishing
on $\mathcal{T}_\delta^h \backslash \Omega_\delta^h$ are defined as follows: for $j = 1, 2, \cdots, n_1 + n_2$,

$$\widetilde{\phi}_j(\mathbf{x}) = \begin{cases} \phi_j(\mathbf{x})|_{\Omega_\delta^h}, & \mathbf{x} \in \Omega_\delta^h, \\ 0, & \mathbf{x} \in \mathcal{T}_\delta^h \backslash \Omega_\delta^h. \end{cases}$$

The basis functions of $V_\delta^{c,h}$ which contains all piecewise linear functions vanishing
on $\mathcal{T}_\delta^h \backslash \Omega_\delta^{c,h}$ are defined as follows: for $j = 1, 2, \cdots, p + n_2$,

$$\widetilde{\phi}_j^c(\mathbf{x}) = \begin{cases} \phi_{n_1+j}(\mathbf{x})|_{\Omega_\delta^{c,h}}, & \mathbf{x} \in \Omega_\delta^{c,h}, \\ 0, & \mathbf{x} \in \mathcal{T}_\delta^h \backslash \Omega_\delta^{c,h}. \end{cases}$$

The linear CDG space is then defined as

$$V_\delta^h = V_\delta^{0,h} + g_\delta^h,$$

where $g_\delta^h \in V_\delta^{c,h}$ is an approximation of the boundary data g_δ.

The following *conforming* property is satisfied,

$$(3.2) \qquad V_\delta^{0,h} \subset V^0(\widehat{\Omega}_\delta), \quad V_\delta^{c,h} \subset V^c(\widehat{\Omega}_\delta).$$

An element of V_δ^h is continuous on Ω or Ω_δ^c, but possibly discontinuous across $\partial\Omega$. The linear CDG approximation of (3.1) finds $u_\delta^{0,h} \in V_\delta^{0,h}$ such that $\forall w_h \in V_\delta^{0,h}$,

$$(3.3) \qquad -2\int_\Omega w_h(\mathbf{x}) \int_{B_\delta(\mathbf{x})\cap\Omega} \left(u_\delta^{0,h}(\mathbf{y}) - u_\delta^{0,h}(\mathbf{x}) \right) \gamma_\delta(\mathbf{x},\mathbf{y}) d\mathbf{y} d\mathbf{x}$$

$$= \int_\Omega f_\delta(\mathbf{x}) w_h(\mathbf{x}) d\mathbf{x} + 2\int_\Omega w_h(\mathbf{x}) \int_{B_\delta(\mathbf{x})\cap\Omega_\delta^c} \left(g_\delta^h(\mathbf{y}) - u_\delta^{0,h}(\mathbf{x}) \right) \gamma_\delta(\mathbf{x},\mathbf{y}) d\mathbf{y} d\mathbf{x}.$$

Put together, we get $u_\delta^h = u_\delta^{0,h} + g_\delta^h$ as the final CDG approximation of u_δ on $\widehat{\Omega}_\delta$.

In fact, the triangulations for $\widehat{\Omega}_\delta$ are not required to be consistent across the interface, since the continuity across $\partial\Omega$ of functions in the linear CDG space is not enforced (and there is no reason to assume the continuity a priori). So $\overline{\Omega}$ and $\overline{\Omega_\delta^c}$ could be triangulated separately by different mesh sizes (without any restriction when crossing the boundary) to get Ω_δ^h and $\Omega_\delta^{c,H}$. This offers more flexibility to implement compared to the use of consistent meshing. Hence a whole triangulation of $\widehat{\Omega}_\delta$ is given as

$$\mathcal{T}_\delta^{h,H} = \Omega_\delta^h \cup \Omega_\delta^{c,H},$$

which is called a non-consistent triangulation of $\widehat{\Omega}_\delta$. Thus we define

$$V_\delta^{h,H} = V_\delta^{0,h} + g_\delta^H,$$

where $g_\delta^H \in V_\delta^{c,H}$ is an approximation of g_δ. In this case, the corresponding linear CDG approximation for (3.1) finds $u_\delta^{0,h} \in V_\delta^{0,h}$ such that (3.3) (replacing g_δ^h by g_δ^H) holds for any $w_h \in V_\delta^{0,h}$. And $u_\delta^{h,H} = u_\delta^{0,h} + g_\delta^H$ is the final CDG approximation of u_δ. We assume that $\max\{h, H\} < \delta$ for convenience, which is particularly beneficial when dealing with issues related to VC, because $H < \delta$ can help avoid potential complications in describing the VC discretization.

3.2. **The CDG approximation for the nonlocal problem with spherical interaction neighborhoods.** In [19], the linear CDG method has been shown to yield an optimal convergence rate with respect to the mesh size for some integrable kernels for fixed δ. However, the dependence of error estimate on δ has not been discussed so far. To analyze this dependence, we begin with the following lemma.

Lemma 3.1. [1, 28] *Assume that the family of kernels $\{\gamma_\delta\}$ satisfies the conditions (1.3) and (1.4). Then there exist constants $\delta_0 > 0$, $C_5 > 0$ and $C_6 > 0$ such that for all $0 < \delta \le \delta_0$ and $v \in V^0(\widehat{\Omega}_\delta)$, it holds*

$$(3.4) \qquad C_5 \|v\|_{L^2(\Omega)} \le \|v\|_\delta \le C_6 \delta^{-1} \|v\|_{L^2(\Omega)},$$

where the constants C_5 and C_6 are all independent of δ.

Notice that the original lemma in [1] states that for general d dimensional setting

$$\widetilde{C}_5 \delta^{d/2+1} \|v\|_{L^2(\Omega)} \le \|v\|_\delta \le \widetilde{C}_6 \delta^{d/2} \|v\|_{L^2(\Omega)},$$

under the assumption $\widetilde{\gamma}_\delta(\|\mathbf{z}\|_2) = 1$ instead of the last condition in (1.4), however, the two lemmas are equivalent. The corresponding vector-valued version of the first inequality of (3.4) is proven in [25, Proposition 5.3].

As stated in [1, Remark 2.5], the first inequality of (3.4) can be extended, as done in [2, Proposition 2.5], to the estimate

$$\widehat{C}_5 \|v\|_{L^2(\widehat{\Omega}_\delta)} \le \|v\|_\delta + \int_{S_{-1}} |v(\mathbf{x})|^2 d\mathbf{x}, \tag{3.5}$$

for functions $v \in L^2(\widehat{\Omega}_\delta)$ which do not necessarily vanish on Ω_δ^c, where

$$S_{-1} := \{\mathbf{x} \in \Omega_\delta^c : \text{dist}(\mathbf{x}, \partial\widehat{\Omega}_\delta) \le \delta/2\},$$

while the first inequality of (3.4) can be deduced from (3.5) with the homogeneous Dirichlet condition on Ω_δ^c assumed. This result also coincides with the classical Poincaré's inequality.

Similar to the proof for the error estimate in the $\|\cdot\|_\delta$ norm in Theorem 2.2, we can derive the relationship between the two norms $\|v\|_\delta$ and $\|v\|_{C(\Omega)} + \|v\|_{C(\Omega_\delta^c)}$.

Lemma 3.2. *Assume that the family of kernels $\{\gamma_\delta\}$ satisfies (1.3), (1.4) and (2.1). Then*

$$\|v\|_\delta \lesssim \delta^{-1}(\|v\|_{C(\Omega)} + \|v\|_{C(\Omega_\delta^c)}), \quad \forall v \in C_b(\Omega) \cap C_b(\Omega_\delta^c).$$

To separate the influence due to the discretization of VC, we introduce an intermediate problem which finds

$$u_\delta^* \in V^0(\widehat{\Omega}_\delta) + g_\delta^h$$

such that

$$-\mathcal{L}_\delta u_\delta^*(\mathbf{x}) = f_\delta(\mathbf{x}) \text{ on } \Omega. \tag{3.6}$$

Theorem 3.3. *Assume that the conditions of Theorem 2.2 hold. Let u_δ and u_δ^h be the solutions of (3.1) and (3.3), respectively. Then*

$$\left\|u_\delta - u_\delta^h\right\|_\delta \lesssim \delta^{(3+\mu)/2} + \delta^{-1}h^2, \tag{3.7}$$

$$\left\|u_\delta - u_\delta^h\right\|_{L^2(\Omega)} \lesssim \delta^{(3+\mu)/2} + \delta^{-1}h^2. \tag{3.8}$$

Proof. By (1.2) and (3.6) one has

$$\mathcal{L}_\delta \left(u_\delta - u_\delta^*\right)(\mathbf{x}) = 0, \ \mathbf{x} \in \Omega. \tag{3.9}$$

The direct application of nonlocal maximum principle to (3.9) produces

$$\|u_\delta - u_\delta^*\|_{C(\Omega)} \lesssim \left\|g_\delta - g_\delta^h\right\|_{C(\Omega_\delta^c)} \lesssim h^2 \|g_\delta\|_{C^2(\Omega_\delta^c)}. \tag{3.10}$$

By the generalized nonlocal Green's first identity ([14]) and (3.9) we get

$$\|u_\delta - u_\delta^*\|_\delta^2 = \int_{\Omega_\delta^c} (u_\delta^*(\mathbf{x}) - u_\delta(\mathbf{x})) \int_{\widehat{\Omega}_\delta} (u_\delta(\mathbf{y}) - u_\delta^*(\mathbf{y}) - u_\delta(\mathbf{x}) + u_\delta^*(\mathbf{x})) \gamma_\delta(\mathbf{x}, \mathbf{y}) d\mathbf{y} d\mathbf{x}$$

$$= \int_{\Omega_\delta^c} (g_\delta^h(\mathbf{x}) - g_\delta(\mathbf{x})) \int_{\widehat{\Omega}_\delta} \left(u_\delta(\mathbf{y}) - u_\delta^*(\mathbf{y}) - g_\delta(\mathbf{x}) + g_\delta^h(\mathbf{x})\right) \gamma_\delta(\mathbf{x}, \mathbf{y}) d\mathbf{y} d\mathbf{x}$$

$$\lesssim |\Omega_\delta^c| \cdot \left\|g_\delta - g_\delta^h\right\|_{C(\Omega_\delta^c)} \cdot \left(\|u_\delta - u_\delta^*\|_{C(\Omega)} + \left\|g_\delta - g_\delta^h\right\|_{C(\Omega_\delta^c)}\right) \cdot G(\gamma_\delta)$$

$$\lesssim \delta \cdot h^2 \|g_\delta\|_{C^2(\Omega_\delta^c)} \cdot h^2 \|g_\delta\|_{C^2(\Omega_\delta^c)} \cdot \delta^{-2} \approx \delta^{-1}h^4.$$

Thus

$$\|u_\delta - u_\delta^*\|_\delta \lesssim \delta^{-1/2}h^2. \tag{3.11}$$

Since $V_\delta^{0,h} \subset V^0(\widehat{\Omega}_\delta)$ as pointed out in (3.2), then for all $w_h \in V_\delta^{0,h}$, it holds

$$-\int_\Omega w_h(\mathbf{x}) \mathcal{L}_\delta u_\delta^*(\mathbf{x}) d\mathbf{x} = \int_\Omega w_h(\mathbf{x}) f_\delta(\mathbf{x}) d\mathbf{x},$$

which, together with (3.3) and the nonlocal Green's first identity [14] leads to

$$\left(u_\delta^* - u_\delta^h, w_h \right)_\delta = 0, \ \forall w_h \in V_\delta^{0,h}.$$

Thus we get the following estimate: for all $v_h \in V_\delta^h$,

$$\left\| u_\delta^* - u_\delta^h \right\|_\delta^2 = \left(u_\delta^* - u_\delta^h, u_\delta^* - u_\delta^h \right)_\delta = \left(u_\delta^* - u_\delta^h, u_\delta^* - v_h \right)_\delta \le \left\| u_\delta^* - u_\delta^h \right\|_\delta \left\| u_\delta^* - v_h \right\|_\delta,$$

where the crucial relation $u_\delta^h - v_h \in V_\delta^{0,h}$ is used. Then

$$(3.12) \qquad \left\| u_\delta^* - u_\delta^h \right\|_\delta \le \left\| u_\delta^* - v_h \right\|_\delta, \ \forall v_h \in V_\delta^h.$$

Let $v_h = I_h \widetilde{u}_0 \in V_\delta^h$ be the piecewise linear interpolant of $\widetilde{u}_0$ on $\mathcal{T}_\delta^h$. By (2.3), Lemma 3.2, (3.11), and the error estimate for the Lagrangian interpolation, we have

$$
\begin{aligned}
(3.13) \qquad \left\| u_\delta^* - u_\delta^h \right\|_\delta &\le \left\| u_\delta^* - I_h \widetilde{u}_0 \right\|_\delta \\
&\le \left\| \widetilde{u}_0 - I_h \widetilde{u}_0 \right\|_\delta + \left\| u_\delta^* - u_\delta \right\|_\delta + \left\| u_\delta - \widetilde{u}_0 \right\|_\delta \\
&\le C\delta^{-1} \left\| \widetilde{u}_0 - I_h \widetilde{u}_0 \right\|_{C(\widehat{\Omega}_\delta)} + C\delta^{-1/2} h^2 + C\delta^{(3+\mu)/2} \\
&\le C\delta^{-1} h^2 \left\| \widetilde{u}_0 \right\|_{C^2(\widehat{\Omega}_\delta)} + C\delta^{-1/2} h^2 + C\delta^{(3+\mu)/2} \\
&\lesssim \delta^{(3+\mu)/2} + \delta^{-1} h^2.
\end{aligned}
$$

This, together with (3.11), leads to (3.7).

Since $u_\delta^* - u_\delta^h \in V^0(\widehat{\Omega}_\delta)$, then by Lemma 3.1, we have

$$(3.14) \qquad \left\| u_\delta^* - u_\delta^h \right\|_{L^2(\Omega)} = \left\| u_\delta^* - u_\delta^h \right\|_{L^2(\widehat{\Omega}_\delta)} \lesssim \left\| u_\delta^* - u_\delta^h \right\|_\delta \lesssim \delta^{(3+\mu)/2} + \delta^{-1} h^2.$$

This, together with (3.10), leads to

$$\left\| u_\delta - u_\delta^h \right\|_{L^2(\Omega)} \le \left\| u_\delta - u_\delta^* \right\|_{L^2(\Omega)} + \left\| u_\delta^* - u_\delta^h \right\|_{L^2(\Omega)} \lesssim \delta^{(3+\mu)/2} + \delta^{-1} h^2,$$

this is (3.8), the proof is complete. $\qquad\square$

Remark 3.4. The convergence rates (3.8) is possibly not sharp, which is due to the inequality (3.14) used. As we know, when FEMs are used to discretize a PDE, the Aubin-Nitsche technique often remains valid. Thus, the discretization error in the L^2 norm tends to exhibit a higher order than that in the H^1 semi-norm with respect to the mesh size. Although there is no proof of its analog in the nonlocal problem setting with an integrable kernel (due to the lack of regularity pick-up), we are able to numerically observe this phenomenon from the numerical results in Section 5. That is, the L^2 norm of the discretization error exhibits a higher order with respect to the horizon parameter than the energy norm.

3.3. The CDG approximation for the nonlocal problem with polygonal interaction neighborhoods.

The linear CDG approximation for the nonlocal problem (2.7) finds $u_{\delta,n_\delta}^{0,h} \in V_\delta^{0,h}$ such that for all $w_h \in V_\delta^{0,h}$,

$$(3.15) \qquad -2 \int_\Omega w_h(\mathbf{x}) \int_\Omega \left(u_{\delta,n_\delta}^{0,h}(\mathbf{y}) - u_{\delta,n_\delta}^{0,h}(\mathbf{x}) \right) \gamma_{\delta,n_\delta}(\mathbf{x},\mathbf{y}) d\mathbf{y} d\mathbf{x}$$

$$= \int_\Omega f_\delta(\mathbf{x}) w_h(\mathbf{x}) d\mathbf{x} + 2 \int_\Omega w_h(\mathbf{x}) \int_{\Omega_\delta^c} \left(g_\delta^h(\mathbf{y}) - u_{\delta,n_\delta}^{0,h}(\mathbf{x}) \right) \gamma_{\delta,n_\delta}(\mathbf{x},\mathbf{y}) d\mathbf{y} d\mathbf{x},$$

and $u_{\delta,n_\delta}^h = u_{\delta,n_\delta}^{0,h} + g_\delta^h$ is the final approximation of u_{δ,n_δ}. Note that since $\mathcal{T}_\delta^h$ is quasi-uniform, then

$$(3.16) \qquad n_\delta \sim \delta/h.$$

We introduce the intermediate problem which finds $u_{\delta,n_\delta}^* \in V^0(\widehat{\Omega}_\delta) + g_\delta^h$ such that

$$-\mathcal{L}_{\delta,n_\delta} u_{\delta,n_\delta}^* = f_\delta.$$

Using the similar argument in Theorem 3.3, we have the following error estimate.

Theorem 3.5. *If the conditions of Theorem 2.9 hold. We have*

$$(3.17) \qquad \|u_{\delta,n_\delta} - u_{\delta,n_\delta}^h\|_{\delta,n_\delta} \lesssim \delta^{(3+\mu)/2} + \delta^{-1}h^2 + \delta^{-\lambda-1}h^\lambda,$$

$$(3.18) \qquad \|u_{\delta,n_\delta} - u_{\delta,n_\delta}^h\|_{L^2(\Omega)} \lesssim \delta^{(3+\mu)/2} + \delta^{-1}h^2 + \delta^{-\lambda-1}h^\lambda.$$

Proof. Similar to the derivation in Theorem 3.3, we have

$$(3.19) \qquad \|u_{\delta,n_\delta} - u_{\delta,n_\delta}^*\|_{C(\Omega)} \lesssim \|g_\delta - g_\delta^h\|_{C(\Omega_\delta^c)} \le Ch^2 \|g_\delta\|_{C^2(\Omega_\delta^c)},$$

$$(3.20) \qquad \|u_{\delta,n_\delta} - u_{\delta,n_\delta}^*\|_{\delta,n_\delta} \le C\delta^{-1/2}h^2.$$

Since $n_\delta \to \infty$ as $\delta \to 0$, by (2.8), Lemma 3.2 and (2.22), we have

$$(3.21) \qquad \|u_{\delta,n_\delta}^* - u_{\delta,n_\delta}^h\|_{\delta,n_\delta} \le \|u_{\delta,n_\delta}^* - I_h \widetilde{u}_0\|_{\delta,n_\delta}$$

$$\le \|u_{\delta,n_\delta}^* - u_{\delta,n_\delta}\|_{\delta,n_\delta} + \|\widetilde{u}_0 - I_h \widetilde{u}_0\|_{\delta,n_\delta} + \|u_{\delta,n_\delta} - \widetilde{u}_0\|_{\delta,n_\delta}$$

$$\le C\delta^{-1/2}h^2 + C\delta^{-1}\|\widetilde{u}_0 - I_h \widetilde{u}_0\|_{C(\widehat{\Omega}_\delta)} + \|u_{\delta,n_\delta} - \widetilde{u}_0\|_{\delta,n_\delta}$$

$$\le C\delta^{-1/2}h^2 + C\delta^{-1}h^2\|\widetilde{u}_0\|_{C^2(\widehat{\Omega}_\delta)} + C\delta^{-1}n_\delta^{-\lambda} + Cn_\delta^{-\lambda} + C\delta^{(3+\mu)/2}$$

$$\lesssim \delta^{(3+\mu)/2} + \delta^{-1}h^2 + \delta^{-1}n_\delta^{-\lambda}.$$

This, together with (3.20) and (3.16), leads to (3.17). By the uniform Poincaré's inequality for the norm $\|\cdot\|_\delta$, (2.8) and (3.19), we get (3.18). $\qquad\square$

4. Error estimates between the nonlocal discrete solutions and the local exact solution

We now combine the error estimates in Section 2 and Section 3 to derive the error estimate between the nonlocal discrete solutions and the local exact solution.

First, by combining Theorem 2.2 and Theorem 3.3 we get the following theorem.

Theorem 4.1. *Suppose $u_0 \in C_b^4(\Omega)$ is the solution of the local problem (1.5), the family of kernels $\{\gamma_\delta\}$ satisfies (1.3), (1.4) and (2.1). If $\widetilde{u}_0$ is a C^4 extension of*

u_0, u_δ^h is the linear CDG approximation of the nonlocal problem (1.2) *under the condition* (2.2), *then it holds that*

$$(4.1) \qquad \left\|\widetilde{u}_0 - u_\delta^h\right\|_\delta = \left\|\widetilde{u}_0 - u_\delta + u_\delta - u_\delta^h\right\|_\delta \lesssim \delta^{(3+\mu)/2} + \delta^{-1}h^2,$$

$$(4.2) \qquad \left\|u_0 - u_\delta^h\right\|_{L^2(\Omega)} = \left\|u_0 - u_\delta + u_\delta - u_\delta^h\right\|_{L^2(\Omega)} \lesssim \delta^{(3+\mu)/2} + \delta^{-1}h^2.$$

To make the analysis related to polygonal approximation concrete, we take the constant kernel (2.27) as an illustrative example ($\lambda = 2$) and adopt *nocaps* as an approximation of the spherical neighborhood, that is, an approximation using the inscribed polygon of the Euclidean disc. We note that the analysis can be extended to other types of kernels listed in Section 2.3 and other types of polygonal approximations. Since $\lambda = 2$ and (3.16), together with Theorem 2.9 and Theorem 3.5 we get the following theorem.

Theorem 4.2. *Suppose $u_0 \in C_b^4(\Omega)$ is the solution of the local problem* (1.5), *the family of kernels $\{\gamma_\delta\}$ satisfies* (1.3), (1.4) *and* (2.1). *$\{B_{\delta,n_\delta^\times}\}$ is a weakly quasi-uniform family of inscribed polygons. $\widetilde{u}_0$ is a C^4 extension of u_0 and u_{δ,n_δ}^h is the linear CDG approximation of the nonlocal problem* (2.7) *under the condition* (2.2). *If* (2.20), *then it holds that*

$$(4.3) \qquad \|\widetilde{u}_0 - u_{\delta,n_\delta}^h\|_{\delta,n_\delta} \lesssim \delta^{(3+\mu)/2} + \delta^{-1}h^2 + \delta^{-\lambda-1}h^\lambda \sim \delta^{(3+\mu)/2} + \delta^{-3}h^2,$$

$$(4.4) \qquad \|u_0 - u_{\delta,n_\delta}^h\|_{L^2(\Omega)} \lesssim \delta^{(3+\mu)/2} + \delta^{-1}h^2 + \delta^{-\lambda-1}h^\lambda \sim \delta^{(3+\mu)/2} + \delta^{-3}h^2.$$

5. Numerical experiment

We first consider in Section 5.1 the nonlocal problems with the exact right-hand side (RHS) function and VC. Hence the error induced in Theorem 2.2 vanishes. We report the convergence results of *exactcaps* (u_δ^h) and *nocaps* (u_{δ,n_δ}^h) solutions for three cases of parameter setting: fixed horizon parameter, fixed ratio and power function between the horizon parameter and the mesh size. They corresponds to m-convergence, δ-convergence, and δm-convergence for numerical methods of peridynamics defined in [7], respectively. Then in Section 5.2 the nonlocal problems with a perturbed RHS function and VC are discussed.

5.1. Nonlocal problems with an exact RHS function and VC.

Example 5.1. We consider the nonlocal problem (1.2) on the domain $\Omega = (0,1)^2$ with the family of kernels $\{\gamma_\delta\}$ defined by (2.27) in 2D, namely

$$(5.1) \qquad \gamma_\delta(\mathbf{x}, \mathbf{y}) = \begin{cases} 4/\pi/\delta^4, & |\mathbf{x} - \mathbf{y}| \le \delta, \\ 0, & |\mathbf{x} - \mathbf{y}| > \delta. \end{cases}$$

As in [11] the manufactured solution $u_\delta(\mathbf{x}) = x_1^2 x_2 + x_2^2$ is used to obtain the RHS function $f_\delta(\mathbf{x}) = -2(x_2 + 1)$ for $\mathbf{x} \in \Omega$ and VC $g_\delta(\mathbf{x}) = u_\delta(\mathbf{x})$ for $\mathbf{x} \in \Omega_\delta^c$.

The solution of the local problem (1.5) with a RHS function $f_0(\mathbf{x}) = -2(x_2 + 1)$ and boundary function $g_0(\mathbf{x}) = x_1^2 x_2 + x_2^2$ is $u_0(\mathbf{x}) = u_\delta(\mathbf{x})|_\Omega$, while we take

$$\widetilde{u}_0(\mathbf{x}) = x_1^2 x_2 + x_2^2 \text{ for } \mathbf{x} \in \widehat{\Omega}_\delta.$$

In fact in this example $g_\delta = \widetilde{u}_0$ on Ω_δ^c, $f_\delta = f_0$ on Ω holds in Theorem 2.2. Thus $u_\delta = \widetilde{u}_0$ on $\widehat{\Omega}_\delta$, and the term $\delta^{(3+\mu)/2}$ in (4.1) to (4.4) vanishes. Then we report on the errors in different norms of u_δ^h and u_{δ,n_δ}^h against $\widetilde{u}_0$.

5.1.1. *Numerical results for a fixed horizon parameter.* We fix $\delta = 0.4$ as the mesh is refined with a decreasing h, and then study the errors and convergence rates of the *exactcaps* and *nocaps* solutions. For the polygon Ω, the corresponding inter-action domain Ω_δ^c has rounded corners, thus it cannot be fully triangulated into elements with straight sides. As pointed out in [11], Ω_δ^c can be approximated by a polygonal domain with sharp corners to replace the rounded corners while avoiding the extension of the function g_δ. The corresponding (consistent) mesh $\mathcal{T}_\delta^h$ and the solution u_δ^h for $h = 0.05$ are plotted in Figure 3. Since the figure of u_{δ,n_δ}^h is similar to that of u_δ^h, the former is omitted. We also use a non-consistent mesh to obtain u_δ^h, the corresponding mesh and the solution are plotted in Figure 4. Since the solutions of two strategies (using consistent and non-consistent meshes) are rather similar, we take the consistent mesh for later numerical experiments.
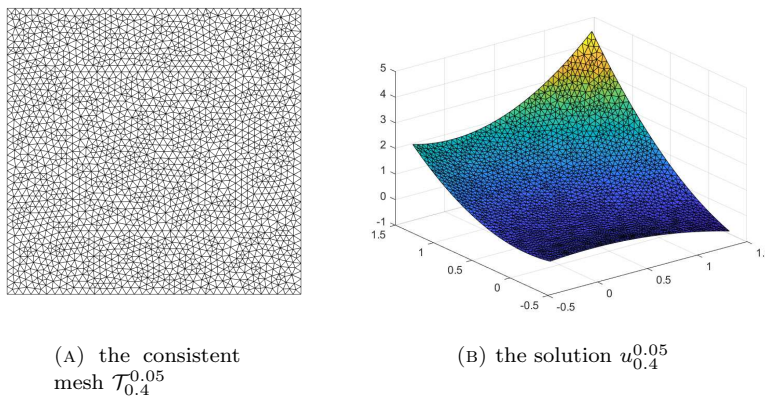

(A) the consistent mesh $\mathcal{T}_{0.4}^{0.05}$

(B) the solution $u_{0.4}^{0.05}$

FIGURE 3. Example 5.1: the consistent mesh and corresponding *exactcaps* solution u_δ^h, $\delta = 0.4$, $h = 0.05$

Panel (B) of Figure 3 shows that the solutions u_δ^h are continuous across $\partial\Omega$. In fact, in this example, they are expected to be continuous since the analytic expression of u_δ is specified in advance. This assertion could not be applied to u_{δ,n_δ}^h since the analytic expression of u_{δ,n_δ} is unknown. In fact, there is a lack of theory so far to ensure the continuity of u_δ across $\partial\Omega$ in general, although the continuity in Ω has been discussed in [19]. Along this line, the continuity across $\partial\Omega$ for u_{δ,n_δ} is also not assured. Due to the definition of the linear CDG space, u_δ^h and u_{δ,n_δ}^h are allowed to be discontinuous across $\partial\Omega$. Here $u_{0.4}^{0.05}$ might appear to be continuous simply because the jumps across $\partial\Omega$ are smaller than the scales of the solution itself. If we zoom in to examine these solutions in greater detail, especially for larger h, the discontinuity can become more visible. For this purpose, we present zoomed plots around point $(1, 1)$ of the solutions u_δ^h and u_{δ,n_δ}^h for $h = \delta$ in Figure 5.

It is seen from Table 1 that the solution u_δ^h has smaller errors in the energy norm than that of u_{δ,n_δ}^h, while the opposite behavior is observed in the case of the L^2 norm. However, we do observe the second-order convergence rates for both methods in both types of norms. This confirms the theoretical results since δ is taken to be a constant in this set of experiments, that is by (4.1) to (4.4) without
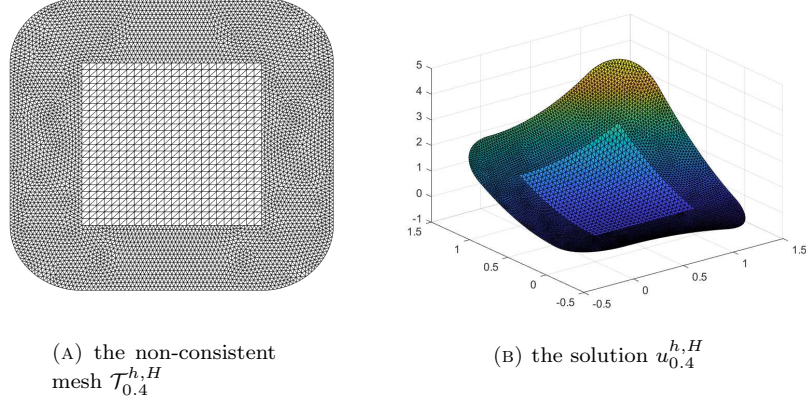
(A) the non-consistent mesh $\mathcal{T}_{0.4}^{h,H}$

(B) the solution $u_{0.4}^{h,H}$

FIGURE 4. Example 5.1: the non-consistent mesh and corresponding solution $u_\delta^{h,H}$, $\delta = 0.4$, $h = 0.05\sqrt{2}$, $H = 3h/8$

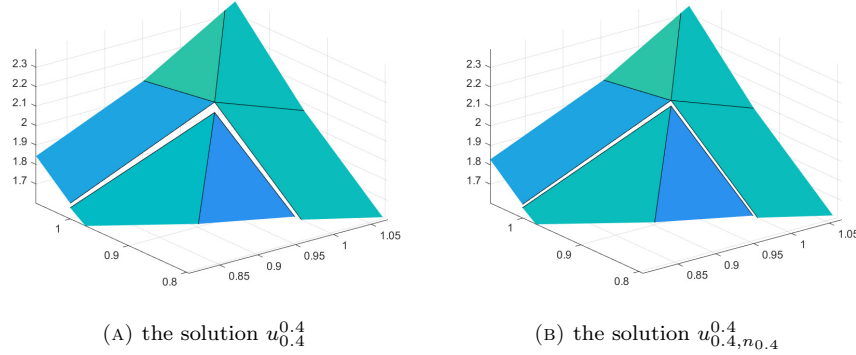(A) the solution $u_{0.4}^{0.4}$

(B) the solution $u_{0.4,n_{0.4}}^{0.4}$

FIGURE 5. Example 5.1: zoom around point $(1,1)$ of u_δ^h and u_{δ,n_δ}^h, $h = \delta = 0.4$

the term $\delta^{(3+\mu)/2}$, the errors in the energy and L^2 norms of u_δ^h and u_{δ,n_δ}^h are of $\delta^{-1}h^2$ and $\delta^{-3}h^2$ order, respectively.

5.1.2. *Numerical results for the case of a fixed ratio between the horizon parameter and the mesh size.* In this part, we fix $m = \delta/h$ as a constant while refining δ. In this case (4.1) and (4.2) without the term $\delta^{(3+\mu)/2}$ turn out as

$$(5.2) \qquad \left\| \widetilde{u}_0 - u_\delta^h \right\|_\delta \lesssim \delta m^{-1},$$

$$(5.3) \qquad \left\| u_0 - u_\delta^h \right\|_{L^2(\Omega)} \lesssim \delta m^{-1}.$$

Table 2 provides errors and convergence rates of *exactcaps* solution u_δ^h against the local exact solution u_0 in the energy norm with $m = 2, 3, 4$, and 5, respectively. The convergence rates all exhibit the first order with respect to δ, which are consistent with (5.2). We also use the same data of errors to calculate the convergence rates

TABLE 1. Example 5.1: errors and convergence rate of nonlocal numerical solutions u_δ^h and u_{δ,n_δ}^h against the local exact solution $\widetilde{u}_0$ in the energy norms and L^2 norms, $\delta = 0.4$

$\frac{\delta}{h}$	Energy norm					L^2 norm			
	$\|\widetilde{u}_0\text{-}u_\delta^h\|_\delta$	Rate	$\|\widetilde{u}_0\text{-}u_{\delta,n_\delta}^h\|_{\delta,n_\delta}$	Rate	$\|\widetilde{u}_0\text{-}u_{\delta,n_\delta}^h\|_\delta$	$\|u_0\text{-}u_\delta^h\|$	Rate	$\|u_0\text{-}u_{\delta,n_\delta}^h\|$	Rate
2^0	6.38e-2	–	1.22e-1	–	1.25e-1	1.58e-2	–	1.40e-2	–
2^1	1.01e-2	2.66	2.51e-2	2.28	2.53e-2	6.11e-3	1.37	2.08e-3	2.75
2^2	2.83e-3	1.84	6.67e-3	1.91	6.69e-3	1.46e-3	2.06	4.65e-4	2.16
2^3	6.49e-4	2.12	1.58e-3	2.07	1.58e-3	3.70e-4	1.98	1.27e-4	1.88
2^4	1.58e-4	2.04	3.95e-4	2.00	3.95e-4	9.14e-5	2.02	3.17e-5	2.00
2^5	3.96e-5	1.99	9.76e-5	2.02	9.76e-5	2.28e-5	2.01	8.11e-6	1.97

TABLE 2. Example 5.1: errors $\|\widetilde{u}_0 - u_\delta^h\|_\delta$ and convergence rates, $\delta = mh$

δ_0/δ	2^0	2^1	2^2	2^3	2^4	2^5
$\delta_0{=}0.4$, $m{=}2$	1.01e-2	5.12e-3	2.43e-3	1.16e-3	5.73e-4	2.84e-4
Rate	–	0.98	1.08	1.07	1.02	1.01
$\delta_0{=}0.6$, $m{=}3$	6.89e-3	3.60e-3	1.72e-3	8.14e-4	4.02e-4	1.98e-4
Rate	–	0.94	1.07	1.08	1.02	1.02
$\delta_0{=}0.8$, $m{=}4$	5.13e-3	2.83e-3	1.30e-3	6.19e-4	3.08e-4	1.51e-4
Rate	–	0.86	1.12	1.07	1.01	1.03
$\delta_0{=}1.0$, $m{=}5$	3.90e-3	2.26e-3	1.02e-3	4.99e-4	2.48e-4	1.21e-4
Rate	–	0.79	1.15	1.03	1.01	1.04

TABLE 3. Example 5.1: errors $\|\widetilde{u}_0 - u_\delta^h\|_\delta$, $\|\widetilde{u}_0 - u_{\delta,n_\delta}^h\|_{\delta,n_\delta}$ and convergence rates, h fixed

h	$\|\widetilde{u}_0 - u_\delta^h\|_\delta$				$\|\widetilde{u}_0 - u_{\delta,n_\delta}^h\|_{\delta,n_\delta}$			
	$\delta = 2h$	$\delta = 3h$	$\delta = 4h$	$\delta = 5h$	$\delta = 2h$	$\delta = 3h$	$\delta = 4h$	$\delta = 5h$
0.2	1.01e-2	6.89e-3	5.13e-3	3.90e-3	2.51e-2	1.37e-2	9.35e-3	7.25e-3
Rate	–	-0.94	-1.03	-1.23	–	-1.49	-1.33	-1.14
0.1	5.12e-3	3.60e-3	2.83e-3	2.26e-3	2.73e-2	1.02e-2	6.67e-3	4.81e-3
Rate	–	-0.87	-0.84	-1.01	–	-2.43	-1.48	-1.47
0.05	2.43e-3	1.72e-3	1.30e-3	1.02e-3	3.55e-2	1.21e-2	5.91e-3	3.83e-3
Rate	–	-0.85	-0.97	-1.09	–	-2.65	-2.49	-1.94
0.025	1.16e-3	8.14e-4	6.19e-4	4.99e-4	6.51e-2	1.77e-2	7.81e-3	4.41e-3
Rate	–	-0.87	-0.95	-0.97	–	-3.21	-2.84	-2.56
0.0125	5.73e-4	4.02e-4	3.08e-4	2.48e-4	1.36e-1	3.66e-2	1.48e-2	7.54e-3
Rate	–	-0.87	-0.93	-0.97	–	-3.24	-3.15	-3.02
0.00625	2.84e-4	1.98e-4	1.51e-4	1.21e-4	2.67e-1	7.06e-2	2.94e-2	1.50e-2
Rate	–	-0.89	-0.94	-0.99	–	-3.28	-3.05	-3.02

with respect to δ for fixed h. To this end, notice that h is constant in each column of Table 2. Thus, we rotate Table 2 90 degrees to get the middle part of Table 3.

It shows nearly -1 order with respect to δ for a fixed h, which coincides with the error estimate (4.1) without the term $\delta^{(3+\mu)/2}$.

TABLE 4. Example 5.1: errors $\|u_0 - u_\delta^h\|_{L^2(\Omega)}$ and convergence rates, $\delta = mh$

δ_0/δ	2^0	2^1	2^2	2^3	2^4	2^5
$\delta_0=0.4$, $m=2$	6.11e-3	1.56e-3	3.61e-4	9.75e-5	2.32e-5	4.92e-6
Rate	–	1.97	2.11	1.89	2.07	2.24
$\delta_0=0.6$, $m=3$	5.97e-3	1.75e-3	4.47e-4	1.08e-4	2.72e-5	7.03e-6
Rate	–	1.77	1.97	2.05	1.99	1.95
$\delta_0=0.8$, $m=4$	5.97e-3	1.46e-3	3.55e-4	1.01e-4	2.38e-5	5.68e-6
Rate	–	2.03	2.04	1.81	2.09	2.07
$\delta_0=1.0$, $m=5$	6.31e-3	1.49e-3	3.84e-4	9.75e-5	2.44e-5	6.07e-6
Rate	–	2.08	1.96	1.98	2.00	2.01

In Table 4 the results in the L^2 norm are reported. The convergence rates show the second order, across the table, which is better than that predicted by (5.3). Furthermore, we hardly observe any obvious drop or growth of errors when δ decreases for fixed h, see the data along each column. The two findings indicate that the error estimate (4.2) is likely not sharp. It seems (4.2) may be improved as

$$(5.4) \qquad \left\|u_0 - u_\delta^h\right\|_{L^2(\Omega)} \lesssim \delta^2 + h^2,$$

which suggests the possible validity of the Aubin-Nitsche technique with respect to the horizon parameter, see also Remark 3.4.

Since $\delta = mh$, (4.3) and (4.4) turn out as

$$(5.5) \qquad \|\widetilde{u}_0 - u_{\delta,n_\delta}^h\|_{\delta,n_\delta} \lesssim \delta^2 + \delta^{-3}h^2 \approx \delta^{-1}m^{-2},$$

$$(5.6) \qquad \|u_0 - u_{\delta,n_\delta}^h\|_{L^2(\Omega)} \lesssim \delta^2 + \delta^{-3}h^2 \approx \delta^{-1}m^{-2}.$$

TABLE 5. Example 5.1: errors $\|\widetilde{u}_0 - u_{\delta,n_\delta}^h\|_{\delta,n_\delta}$ and convergence rates, $\delta = mh$

δ_0/δ	2^0	2^1	2^2	2^3	2^4	2^5
$\delta_0=0.4$, $m=2$	2.51e-2	2.73e-2	3.55e-2	6.51e-2	1.36e-1	2.67e-1
Rate	–	-0.12	-0.38	-0.87	-1.06	-0.97
$\delta_0=0.6$, $m=3$	1.37e-2	1.02e-2	1.21e-2	1.77e-2	3.66e-2	7.06e-2
Rate	–	0.43	-0.25	-0.55	-1.05	-0.95
$\delta_0=0.8$, $m=4$	9.35e-3	6.67e-3	5.91e-3	7.81e-3	1.48e-2	2.94e-2
Rate	–	0.49	0.17	-0.40	-0.92	-0.99
$\delta_0=1.0$, $m=5$	7.25e-3	4.81e-3	3.83e-3	4.41e-3	7.54e-3	1.50e-2
Rate	–	0.59	0.33	-0.20	-0.77	-0.99

Table 5 provides errors and convergence rates of *nocaps* solution u_{δ,n_δ}^h against the local exact solution u_0 in the energy norm. The convergence rates are near -1 order with respect to δ for decreasing δ under the setting $\delta = mh$ (as seen for each row), which coincides with (5.5). We also calculate the convergence rates with respect to δ for fixed h, see the right part of Table 3. They show nearly -3

order, which coincides with (4.3) without the term $\delta^{(3+\mu)/2}$. In Table 6 the results in the L^2 norm are reported. On the one hand, errors stabilize gradually around a certain value when δ decreases under the setting $\delta = mh$, which is better than that predicted by (5.6). On the other hand, the rates show nearly -2 order with respect to δ for fixed h (if computed along each column, similar to Table 3, the numerical values are omitted to save space). The two findings indicate that the error estimate (4.4) is not sharp, and a possible improvement of (4.4) may be given by

$$(5.7) \qquad \|u_0 - u_{\delta,n_\delta}^h\|_{L^2(\Omega)} \lesssim \delta^{-2}h^2 + \delta^2 + h^2.$$

TABLE 6. Example 5.1: errors $\|u_0 - u_{\delta,n_\delta}^h\|_{L^2(\Omega)}$ and convergence rates, $\delta = mh$

δ_0/δ	2^0	2^1	2^2	2^3	2^4	2^5
$\delta_0=0.4$, $m=2$	2.08e-3	3.06e-3	3.52e-3	2.70e-3	2.20e-3	2.49e-3
Rate	–	-0.56	-0.20	0.38	0.30	-0.18
$\delta_0=0.6$, $m=3$	2.68e-3	8.36e-4	1.66e-3	1.44e-3	1.21e-3	1.08e-3
Rate	–	1.68	-0.99	0.21	0.25	0.16
$\delta_0=0.8$, $m=4$	3.39e-3	4.65e-4	7.63e-4	8.21e-4	7.33e-4	7.20e-4
Rate	–	2.87	-0.71	-0.11	0.16	0.03
$\delta_0=1.0$, $m=5$	3.76e-3	4.95e-4	4.64e-4	5.45e-4	4.71e-4	4.63e-4
Rate	–	2.93	0.09	-0.23	0.21	0.02

5.1.3. *Numerical results for power law between the horizon parameter and the mesh size.* The sharpness of the estimates (4.1) and (4.3) has been discussed to some extent in the two subsections above. Here we further verify this sharpness by setting $h = O\left(\delta^\beta\right)$. By (4.1) and (4.2) without the term $\delta^{(3+\mu)/2}$, it is expected that

$$(5.8) \qquad \|\widetilde{u}_0 - u_\delta^h\|_\delta \lesssim \delta^{-1}h^2 \sim \delta^{2\beta-1}, \quad \|u_0 - u_\delta^h\|_{L^2(\Omega)} \lesssim \delta^{-1}h^2 \sim \delta^{2\beta-1}.$$

The errors for $\beta = 1.1, \cdots, 2.0$ are plotted in Figure 6. Here δ is reduced to two-thirds of the previous step each time. Due to the increasing demand on the CPU time as β increases, we take fewer δ refinement for larger β. In (A), the errors versus δ in the energy norm are plotted. We find that the convergence rates are of $2\beta - 1$ order which is consistent with the estimate in the energy norm in (5.8). In (B) the errors in the L^2 norm show the 2β order, which indicates again (4.2) may be improved as (5.4).

Since $h = O\left(\delta^\beta\right)$, (4.3) and (4.4) turn out to be given by

$$(5.9) \qquad \|\widetilde{u}_0 - u_{\delta,n_\delta}^h\|_{\delta,n_\delta} \lesssim \delta^{2\beta-3}, \quad \|u_0 - u_{\delta,n_\delta}^h\|_{L^2(\Omega)} \lesssim \delta^{2\beta-3}.$$

We plot the results of u_{δ,n_δ}^h in Figure 7. The errors versus δ in the energy norm are plotted in (A). The convergence rates show nearly $2\beta - 3$ order which coincides with the estimate in the energy norm in (5.9). It is worth mentioning that errors in the energy norm decrease monotonically only for $\beta > 1.5$. In (B) the errors in the L^2 norm show nearly $2\beta - 2$ order which again suggests (4.4) be improved as (5.7).
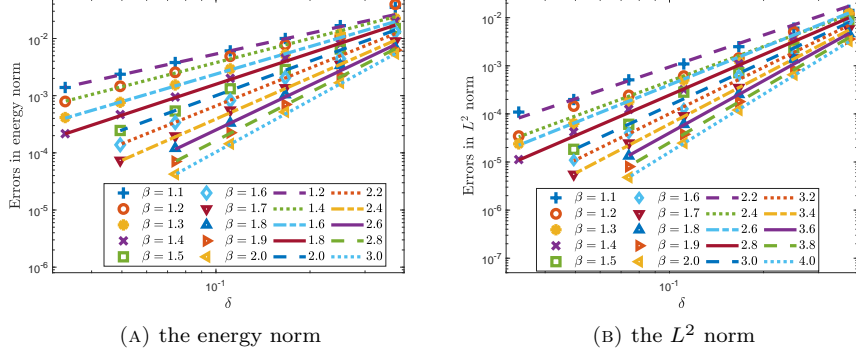
(A) the energy norm

(B) the L^2 norm

FIGURE 6. Example 5.1: errors and convergence rates for *exact-caps* solution u_δ^h against the local exact solution u_0 under the setting $h = O\left(\delta^\beta\right)$, $\beta \in (1, 2]$
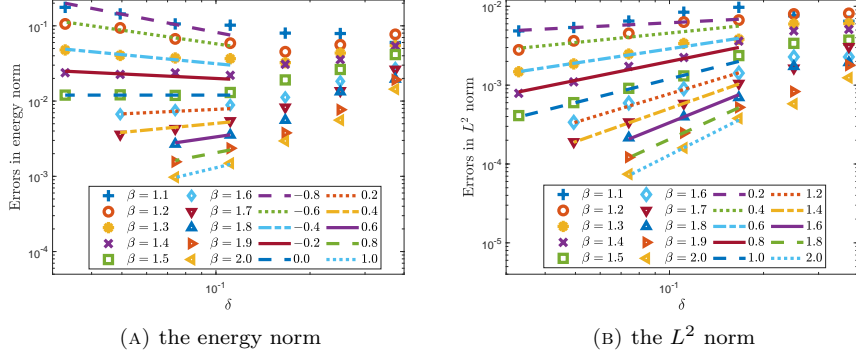

(A) the energy norm

(B) the L^2 norm

FIGURE 7. Example 5.1: errors in different norms for *nocaps* solution u_{δ,n_δ}^h against the local exact solution u_0 under the setting $h = O\left(\delta^\beta\right)$, $\beta \in (1, 2]$

5.2. Nonlocal problems with a perturbed RHS function and VC.

Example 5.2. We consider nonlocal problems (1.2) on the domain $\Omega = (0,1)^2$ with the family of kernels $\{\gamma_\delta\}$ defined by (5.1). We set the RHS function as

$$(5.10) \qquad f_\delta(\mathbf{x}) = -2(x_2 + 1) + \delta^2 e^{x_1^2 + 3x_2^2}, \ \text{for } \mathbf{x} \in \Omega,$$

and the following two kinds of VCs

$$(5.11) \qquad g_\delta(\mathbf{x}) = x_1^2 x_2 + x_2^2 + \delta^2 \sin(x_1 - 2x_2), \ \text{for } \mathbf{x} \in \Omega_\delta^c,$$

$$(5.12) \qquad g_\delta(\mathbf{x}) = x_1^2 x_2 + x_2^2 + \delta^3 \sin(x_1 - 2x_2), \ \text{for } \mathbf{x} \in \Omega_\delta^c,$$

which satisfy (2.2) with $\mu = 0$ and $\mu = 1$, respectively. The corresponding local problem is the same as Example 5.1. Here the nonlocal solutions u_δ and u_{δ,n_δ} are all discontinuous across $\partial\Omega$.

Most numerical results and findings here are similar to those in Section 5.1, so we do not repeat such discussions and only show the numerical results for the case of a fixed ratio between the horizon parameter and the mesh size. Tables 7 and 8 provide the results of *exactcaps* and *nocaps* solutions with $m = 2$, for VCs (5.11) and (5.12), respectively. The convergence rates of u_δ^h for both VCs against $\widetilde{u}_0$ in the L^2 norm show second order, which is similar to the case $m = 2$ in Table 4.

TABLE 7. Example 5.2: errors and convergence rate of nonlocal numerical solutions u_δ^h and u_{δ,n_δ}^h with VC (5.11) against the local exact solution $\widetilde{u}_0$, $\delta_0 = 0.4$, $\delta = 2h$

δ_0/δ	Energy norm				L^2 norm			
	$\|\widetilde{u}_0 - u_\delta^h\|_\delta$	Rate	$\|\widetilde{u}_0\text{-}u_{\delta,n_\delta}^h\|_{\delta,n_\delta}$	Rate	$\|u_0 - u_\delta^h\|$	Rate	$\|u_0\text{-}u_{\delta,n_\delta}^h\|$	Rate
2^0	2.80e-1	–	2.74e-1	–	5.83e-2	–	5.61e-2	–
2^1	1.25e-1	1.17	1.29e-1	1.09	1.49e-2	1.97	1.54e-2	1.86
2^2	5.15e-2	1.28	6.46e-2	0.99	4.08e-3	1.87	5.74e-3	1.42
2^3	1.96e-2	1.40	6.93e-2	-1.01	1.06e-3	1.94	2.94e-3	0.97
2^4	7.20e-3	1.44	1.36e-1	-0.97	2.73e-4	1.96	2.19e-3	0.42
2^5	2.60e-3	1.47	2.67e-1	-0.97	6.92e-5	1.98	2.46e-3	-0.16

TABLE 8. Example 5.2: errors and convergence rate of nonlocal numerical solutions u_δ^h and u_{δ,n_δ}^h with VC (5.12) against the local exact solution $\widetilde{u}_0$, $\delta_0 = 0.4$, $\delta = 2h$

δ_0/δ	Energy norm				L^2 norm			
	$\|\widetilde{u}_0 - u_\delta^h\|_\delta$	Rate	$\|\widetilde{u}_0\text{-}u_{\delta,n_\delta}^h\|_{\delta,n_\delta}$	Rate	$\|u_0 - u_\delta^h\|$	Rate	$\|u_0\text{-}u_{\delta,n_\delta}^h\|$	Rate
2^0	2.28e-1	–	2.15e-1	–	6.13e-2	–	5.75e-2	–
2^1	4.56e-2	2.32	3.86e-2	2.48	1.10e-2	2.48	7.46e-3	2.95
2^2	1.06e-2	2.10	3.31e-2	2.23	2.40e-3	2.19	1.84e-3	2.02
2^3	2.86e-3	1.90	6.50e-2	-0.98	5.83e-4	2.04	2.36e-3	-0.36
2^4	8.65e-4	1.72	1.36e-1	-1.06	1.42e-4	2.03	2.15e-3	0.13
2^5	3.26e-4	1.41	2.67e-1	-0.98	3.44e-5	2.05	2.51e-3	-0.22

The convergence results of u_{δ,n_δ}^h for both VCs against $\widetilde{u}_0$ in the energy and the L^2 norms exhibit about -1 order and zeroth order, respectively. These results are similar to the corresponding results in Tables 5 and 6 although the rates in Tables 7 and 8 have much larger oscillations. The reason is similar to the seemingly abnormal rates for u_δ^h against $\widetilde{u}_0$ in the energy norm, which can be explained as follows.

For errors of u_δ^h in the energy norm, (4.1) turns out to be

$$(5.13) \qquad\qquad \left\|\widetilde{u}_0 - u_\delta^h\right\|_\delta \leq C_7\delta^{3/2} + C_8\delta$$

$$(5.14) \qquad\qquad \left\|\widetilde{u}_0 - u_\delta^h\right\|_\delta \leq C_7\delta^2 + C_8\delta$$

for VCs (5.11) and (5.12), respectively. However, the convergence rates in Table 7 appear to be $3/2$ order which seems inconsistent with (5.13). The rates in Table 8 have a decreasing trend. They might eventually reach the first order, which would coincide with (5.14). In fact, by (1.6) it holds that

$$\left\|\widetilde{u}_0 - u_\delta^h\right\|_\delta \leq \|u_\delta - \widetilde{u}_0\|_\delta + \left\|u_\delta - u_\delta^h\right\|_\delta = E_1 + E_2.$$

Recall that in Example 5.1 the RHS function and VC are all exact such that $u_\delta(\mathbf{x}) = \widetilde{u}_0(\mathbf{x})$ for $\mathbf{x} \in \widehat{\Omega}_\delta$. So, the term E_1 vanishes, which leads to (5.2). The convergence rate of u_δ^h is stable around the first order (see Table 2), which confirms (5.2). Although the convergence rates in Tables 7 and 8 are greater than the first order, the errors are significantly larger than that in Example 5.1. So, it can be reasonably argued that for the RHS (5.10) together with VCs (5.11) and (5.12), E_1 dominates the total error in the first few steps, and then E_2 takes over (it could be understood that C_7 is larger than C_8). Unfortunately, it is rather computationally demanding to carry out the last step in Tables 7 and 8, that is $\delta_0/\delta = 2^5$. To validate the explanation above, we turn to the simpler 1D counterpart.

Example 5.3. We consider the nonlocal problem (1.2) on the domain $\Omega = (0, 1)$ with the family of kernels $\{\gamma_\delta\}$ defined by (2.27) in 1D case. Set RHS function

$$(5.15) \qquad\qquad f_\delta(x) = -6x + \delta^2 e^x, \text{ for } x \in \Omega,$$

and the following two kinds of VCs

$$(5.16) \qquad\qquad g_\delta(x) = x^3 + \delta^2 \sin(x), \text{ for } x \in \Omega_\delta^c,$$

and

$$(5.17) \qquad\qquad g_\delta(x) = x^3 + \delta^3 \sin(x), \text{ for } x \in \Omega_\delta^c,$$

respectively. The solution of the corresponding local problem (1.5) with $f_0(x) = -6x$ and $g_0(x) = x^3$ is

$$u_0(x) = x^3.$$

The *exactcaps* solution is used to numerically solve the nonlocal problem.

Let $\delta_0 = 0.3$, $m = 3$, we use quasi-uniform meshes obtained from a randomly perturbed uniform mesh. To be specific, set $h = 1/n_1$, then $\{x_i^u = ih : i = 0, 1, \cdots, n_1\}$ is a uniform mesh of $[0, 1]$. The quasi-uniform mesh is obtained by adding a random vector $\varepsilon \in \mathbb{R}^{n_1-1}$ (which obeys the uniform distribution on $[-0.2h, 0.2h]$) to x_i^u to reach $x_i^u + \varepsilon_i$, $i = 1, 2, \cdots, n_1 - 1$. Together with x_0^u and $x_{n_1}^u$, the new mesh grids are constructed as follows

$$(5.18) \qquad x_i = x_i^u + \varepsilon_i, \ i = 1, 2, \cdots, n_1 - 1, \ x_0 = x_0^u, \ x_{n_1} = x_{n_1}^u.$$

We have done over twenty tests of different random perturbations, and the convergence rates are all similar. Thus, instead of listing all of them, we select one test to verify our theoretical analysis. Table 9 provides errors and convergence rates of u_δ^h for RHS (5.15) together with VCs (5.16) and (5.17) in the energy norm. It is seen that, in the first six steps, the convergence results are similar to the counterpart of the 2D case (see Tables 7 and 8). And then, as we expected earlier, the convergence rates approach the first order gradually. We also supply the error in the energy norm of the linear CDG approximation with an exact RHS and VC in boldface for the remaining seven steps. Since the error of u_δ^h with RHS (5.15) and VC (5.17) is very close to that with the exact ones at the seventh step, its convergence rate approaches the first order there. While for the rate with the RHS (5.15) and VC (5.16), it takes more steps to reach the first order.

TABLE 9. Example 5.3: errors in the energy norm and convergence rates for *exactcaps* solution

δ_0/δ	(5.16)	Rate	(5.17)	Rate					
2^0	2.06e-1	–	9.79e-2	–	2^6	3.41e-4	1.49	7.95e-5	0.96	**7.94e-5**
2^1	6.62e-2	1.64	1.90e-2	2.37	2^7	1.25e-4	1.45	3.97e-5	1.00	**3.96e-5**
2^2	2.25e-2	1.56	3.98e-3	2.25	2^8	4.58e-5	1.45	1.93e-5	1.04	**1.93e-5**
2^3	7.72e-3	1.54	1.01e-3	1.98	2^9	1.75e-5	1.39	9.62e-6	1.00	**9.63e-6**
2^4	2.69e-3	1.52	3.46e-4	1.55	2^{10}	7.11e-6	1.30	4.92e-6	0.97	**4.92e-6**
2^5	9.54e-4	1.49	1.55e-4	1.16	2^{11}	3.04e-6	1.23	2.44e-6	1.01	**2.40e-6**
					2^{12}	1.38e-6	1.14	1.22e-6	1.01	**1.20e-6**

TABLE 10. Error estimate in the energy norm and implementation issue for the linear CDG solutions, $\lambda = 2$

Interaction neighborhood	$\left\|u_\sharp - \widetilde{u}_0\right\|_\sharp$ (Con)	$\left\|u_\sharp^h - \widetilde{u}_0\right\|_\sharp$ (Dis)	Implementation cost
Euclidean ball $\sharp = \delta$	δ^2	$\delta^2 + \delta^{-1}h^2$	Demanding
Symmetric polygon $\sharp = (\delta\|n_\delta)$	$\delta^2 + n_\delta^{-2}$	–	Very demanding
Polygon $\sharp = (\delta, n_\delta)$	$\delta^2 + \delta^{-1}n_\delta^{-2}$	$\delta^2 + \delta^{-3}h^2$	Less demanding

6. Concluding remarks

In this work, we estimated, in both energy and L^2 norms, the errors between the linear CDG solutions for some linear nonlocal problems and the solution of the local limit, simultaneously with respect to the horizon parameter and mesh size. Let us summarize in Table 10 the error estimates of the two linear CDG solutions in the energy norm, along with their implementation costs. Here (Con) stands for the continuum level, while (Dis) stands for the discrete level. For the case $\delta|n_\delta$ since it lacks an inner product and the induced norm, the corresponding error estimate on the discrete level is not given while the error estimate on the continuous level is actually measured in $\|\cdot\|_\delta$ norm.

6.1. **Other numerical methods.** Besides the CDG method, error estimates for other types of numerical solutions of nonlocal problems (like mesh-free method, collocation method, quadrature-based finite difference method) against the exact local solution may also be carried out in two steps like in this paper. Step 1 (on the continuum level): the error estimate of the nonlocal solutions with different interaction neighborhoods against the local exact solution, which is almost the same as the derivation in Section 2. Step 2 (on the discrete level): the error estimate of the numerical solutions against the nonlocal exact solution removing the impact by the approximation of interaction neighborhood, which plays the same role as the conforming DG method in Section 3. It should be noted that one does not always need to follow the same 2-step process here; for example in [18], a different 2-step process has been given for Fourier spectral methods of nonlocal Allen-Cahn equation (1D in space). However, for numerical analysis in higher dimensions and with polygonal approximation to the original interaction neighborhood (Euclidean ball), our 2-step analysis could be more applicable.

6.2. **Other nonlocal problems.** We have focused on nonlocal problems with L^1 kernels and Dirichlet-type VCs and piecewise smooth data. The approach can be

extended to Neumann or other types of VCs. One could consider more general kernels that might not be L^1. Theoretically, in such cases, nonlocal problems with nonhomogeneous boundary data can be studied by utilizing analytical findings given in [15]. The discussion on the effect of quadrature on the interaction neighborhoods will be more demanding due to potential singularities of the kernels used, although the modifications to the interaction neighborhoods are done generally away from such singularities. In this sense, we expect similar studies can be carried out. Furthermore, one might study extensions to other nonlocal problems, both nonlocal variational problems and nonlocal dynamical systems for which issues like the convergence of the nonlocal numerical solutions to the exact local continuum limit have also been considered either theoretically or numerically [21, 22, 24, 27, 37, 39, 40].

References

1. Burak Aksoylu and Tadele Mengesha, *Results on nonlocal boundary value problems*, Numerical Functional Analysis and Optimization **31** (2010), no. 12, 1301–1317.
2. F Andreu, José M Mazón, Julio D Rossi, and Julián Toledo, *A nonlocal p-laplacian evolution equation with nonhomogeneous dirichlet boundary conditions*, SIAM Journal on Mathematical Analysis **40** (2009), no. 5, 1815–1851.
3. Fuensanta Andreu-Vaillo, José M Mazón, Julio D Rossi, and J Julián Toledo-Melero, *Nonlocal diffusion problems*, no. 165, American Mathematical Soc., 2010.
4. E Askari, F Bobaru, RB Lehoucq, ML Parks, SA Silling, and O Weckner, *Peridynamics for multiscale materials modeling*, Journal of Physics: Conference Series **125** (2008), no. 1, 012078.
5. Jean Pierre Aubin, *Behavior of the error of the approximate solutions of boundary value problems for linear elliptic operators by galerkin's and finite difference methods*, Annali della Scuola Normale Superiore di Pisa-Scienze Fisiche e Matematiche **21** (1967), no. 4, 599–637.
6. Florin Bobaru and Monchai Duangpanya, *The peridynamic formulation for transient heat conduction*, International Journal of Heat and Mass Transfer **53** (2010), no. 19-20, 4047–4059.
7. Florin Bobaru, Mijia Yang, Leonardo Frota Alves, Stewart A Silling, Ebrahim Askari, and Jifeng Xu, *Convergence, adaptive refinement, and scaling in 1d peridynamics*, International Journal for Numerical Methods in Engineering **77** (2009), no. 6, 852–877.
8. Susanne Brenner and Ridgway Scott, *The mathematical theory of finite element methods*, vol. 15, Springer Science & Business Media, 2007.
9. Antoni Buades, Bartomeu Coll, and Jean-Michel Morel, *Image denoising methods. a new nonlocal principle*, SIAM Review **52** (2010), no. 1, 113–147.
10. Xi Chen and Max Gunzburger, *Continuous and discontinuous finite element methods for a peridynamics model of mechanics*, Computer Methods in Applied Mechanics and Engineering **200** (2011), no. 9, 1237–1250.
11. Marta D'Elia, Max Gunzburger, and Christian Vollmann, *A cookbook for approximating euclidean balls and for quadrature rules in finite element methods for nonlocal problems*, Mathematical Models and Methods in Applied Sciences **31** (2021), no. 8, 1505–1567.
12. Qiang Du, *Nonlocal modeling, analysis and computation*, SIAM, 2019.
13. Qiang Du, Max Gunzburger, Richard B Lehoucq, and Kun Zhou, *Analysis and approximation of nonlocal diffusion problems with volume constraints*, SIAM Review **54** (2012), no. 4, 667–696.
14. ———, *A nonlocal vector calculus, nonlocal volume-constrained problems, and nonlocal balance laws*, Mathematical Models and Methods in Applied Sciences **23** (2013), no. 03, 493–540.
15. Qiang Du, Xiaochuan Tian, Cory Wright, and Yue Yu, *Nonlocal trace spaces and extension results for nonlocal calculus*, Journal of Functional Analysis **282** (2022), no. 12, 109453.
16. Qiang Du, Xiaochuan Tian, and Zhi Zhou, *Nonlocal diffusion models with consistent local and fractional limits*, A^3N^2M: Approximation, Applications, and Analysis of Nonlocal, Nonlinear Models: Proceedings of the 50th John H. Barrett Memorial Lectures, Springer, 2023, pp. 175–213.

17. Qiang Du, Hehu Xie, and Xiaobo Yin, *On the convergence to local limit of nonlocal models with approximated interaction neighborhoods*, SIAM Journal on Numerical Analysis **60** (2022), no. 4, 2046–2068.
18. Qiang Du and Jiang Yang, *Asymptotically compatible fourier spectral approximations of nonlocal allen–cahn equations*, SIAM Journal on Numerical Analysis **54** (2016), no. 3, 1899–1919.
19. Qiang Du and Xiaobo Yin, *A conforming dg method for linear nonlocal models with integrable kernels*, Journal of Scientific Computing **80** (2019), no. 3, 1913–1935.
20. Qiang Du, Jiwei Zhang, and Chunxiong Zheng, *On uniform second order nonlocal approximations to linear two-point boundary value problems*, Communications in Mathematical Sciences **17** (2019), no. 6, 1737–1755.
21. Christian Glusa, Marta D'Elia, Giacomo Capodaglio, Max Gunzburger, and Pavel B Bochev, *An asymptotically compatible coupling formulation for nonlocal interface problems with jumps*, SIAM Journal on Scientific Computing **45** (2023), no. 3, A1359–A1384.
22. Prashant K. Jha and Robert Lipton, *Finite element approximation of nonlocal dynamic fracture models*, Discrete and Continuous Dynamical Systems-Series B **26** (2021), no. 3, 1675.
23. Hwi Lee and Qiang Du, *Second-order accurate dirichlet boundary conditions for linear nonlocal diffusion problems*, Communications in Mathematical Sciences **20** (2022), no. 7, 1815–1837.
24. Wangbo Luo and Yanxiang Zhao, *Asymptotically compatible schemes for nonlocal ohta kawasaki model*, arXiv preprint arXiv:2311.15186 (2023).
25. Tadele Mengesha and Qiang Du, *The bond-based peridynamic system with dirichlet-type volume constraint*, Proceedings of the Royal Society of Edinburgh Section A: Mathematics **144** (2014), no. 1, 161–186.
26. Joachim Nitsche, *Ein kriterium für die quasi-optimalität des ritzschen verfahrens*, Numerische Mathematik **11** (1968), no. 4, 346–348.
27. Marco Pasetto, Zhaoxiang Shen, Marta D'Elia, Xiaochuan Tian, Nathaniel Trask, and David Kamensky, *Efficient optimization-based quadrature for variational discretization of nonlocal problems*, Computer Methods in Applied Mechanics and Engineering **396** (2022), 115104.
28. Augusto C Ponce, *An estimate in the spirit of poincaré's inequality*, Journal of the European Mathematical Society **6** (2004), 1–15.
29. Pablo Seleson and Michael Parks, *On the role of the influence function in the peridynamic theory*, International Journal for Multiscale Computational Engineering **9** (2011), no. 6, 689–706.
30. Stewart A Silling, *Reformulation of elasticity theory for discontinuities and long-range forces*, Journal of the Mechanics and Physics of Solids **48** (2000), no. 1, 175–209.
31. Stewart A Silling and Ebrahim Askari, *A meshfree method based on the peridynamic model of solid mechanics*, Computers & Structures **83** (2005), no. 17-18, 1526–1535.
32. Stewart A Silling and RB Lehoucq, *Peridynamic theory of solid mechanics*, Advances in applied mechanics, vol. 44, Elsevier, 2010, pp. 73–168.
33. Yunzhe Tao, Xiaochuan Tian, and Qiang Du, *Nonlocal diffusion and peridynamic models with neumann type constraints and their numerical approximations*, Applied Mathematics and Computation **305** (2017), 282–298.
34. Xiaochuan Tian and Qiang Du, *Analysis and comparison of different approximations to nonlocal diffusion and linear peridynamic equations*, SIAM Journal on Numerical Analysis **51** (2013), no. 6, 3458–3482.
35. _____, *Asymptotically compatible schemes and applications to robust discretization of nonlocal models*, SIAM Journal on Numerical Analysis **52** (2014), no. 4, 1641–1665.
36. _____, *Asymptotically compatible schemes for robust discretization of parametrized problems with applications to nonlocal models*, SIAM Review **62** (2020), no. 1, 199–227.
37. Nathaniel Trask, Huaiqian You, Yue Yu, and Michael L Parks, *An asymptotically compatible meshfree quadrature rule for nonlocal problems with applications to peridynamics*, Computer Methods in Applied Mechanics and Engineering **343** (2019), 151–165.
38. Jerry Zhijian Yang, Xiaobo Yin, and Jiwei Zhang, *On uniform second-order nonlocal approximations to diffusion and subdiffusion equations with nonlocal effect parameter*, Communications in Mathematical Sciences **20** (2022), no. 2, 359–375.
39. Huaiqian You, XinYang Lu, Nathaniel Trask, and Yue Yu, *An asymptotically compatible approach for neumann-type boundary condition on nonlocal problems*, ESAIM: Mathematical Modelling and Numerical Analysis **54** (2020), no. 4, 1373–1413.

40. Yue Yu, Huaiqian You, and Nathaniel Trask, *An asymptotically compatible treatment of traction loading in linearly elastic peridynamic fracture*, Computer Methods in Applied Mechanics and Engineering **377** (2021), 113691.

41. Xiaoping Zhang, Max Gunzburger, and Lili Ju, *Quadrature rules for finite element approximations of 1d nonlocal problems*, Journal of Computational Physics **310** (2016), 213–236.

42. Yajie Zhang and Zuoqiang Shi, *A second-order nonlocal approximation for poisson model with dirichlet boundary*, Research in the Mathematical Sciences **10** (2023), no. 3, 36.